



European Reviews of Chemical Research

Has been issued since 2014.
ISSN 2312-7708, E-ISSN 2413-7243
2017. 4(1). Issued 2 times a year

EDITORIAL BOARD

- Bekhterev Viktor** – Sochi State University, Sochi, Russian Federation (Editor in Chief)
Mosin Oleg – Moscow State University of Applied Biotechnology, Moscow, Russian Federation (Deputy Editor-in-Chief)
Kuvshinov Gennadiy – Sochi State University, Sochi, Russian Federation
Elyukhin Vyacheslav – Center of Investigations and Advanced Education, Mexico, Mexico
Kestutis Baltakys – Kaunas University of Technology, Kaunas, Lithuania
Mamardashvili Nugzar – G.A. Krestov Institute of Solution Chemistry of the Russian Academy of Sciences, Ivanovo, Russian Federation
Maskaeva Larisa – Ural Federal University, Ekaterinburg, Russian Federation
Md Azree Othuman Mydin – Universiti Sains Malaysia, Penang, Malaysia
Navrotskii Aleksandr – Volgograd State Technical University, Volgograd, Russian Federation
Ojovan Michael – Imperial College London, London, UK

Journal is indexed by: **CrossRef** (UK), **Electronic scientific library** (Russia), **Journal Index** (USA), **Open Academic Journals Index** (Russia), **ResearchBib** (Japan), **Scientific Indexing Services** (USA)

All manuscripts are peer reviewed by experts in the respective field. Authors of the manuscripts bear responsibility for their content, credibility and reliability.

Editorial board doesn't expect the manuscripts' authors to always agree with its opinion

Postal Address: 1367/4, Stara Vajnorska str., Bratislava, Slovak Republic, Nove Mesto, 831 04
Release date 15.06.17.
Format 21 × 29,7/4.

Website: <http://ejournal14.com/en/index.html> Headset Georgia.
E-mail: evr2010@rambler.ru
Founder and Editor: Academic Publishing House Researcher s.r.o. Order № 110.

European Reviews of Chemical Research

2017

Is. 1



European Reviews of Chemical Research

European Reviews of Chemical Research

2017

Is 1

Издается с 2014 г.
ISSN 2312-7708, E-ISSN 2413-7243
2017. 4(1). Выходит 2 раза в год.

РЕДАКЦИОННЫЙ СОВЕТ

Бехтерев Виктор – Сочинский государственный университет, Сочи, Российская Федерация (Главный редактор)

Мосин Олег – Московский государственный университет прикладной биотехнологии, Москва, Российская Федерация (Заместитель гл. редактора)

Кувшинов Геннадий – Сочинский государственный университет, Сочи, Российская Федерация

Елюхин Вячеслав – Центр исследований и передового обучения, Мехико, Мексика

Кястутис Балтакис – Каунасский технологический университет, Литва

Мамардашвили Нузгар – Институт химии растворов им. Г.А. Крестова РАН, Иваново, Российская Федерация

Маскаева Лариса – Уральский федеральный университет им. первого Президента России Б.Н. Ельцина, Екатеринбург, Российская Федерация

Мд Азри Отхуман Мудин – Университет Малайзии, Пенанг, Малайзия

Навроцкий Александр – Волгоградский государственный технический университет, Волгоград, Российская Федерация

Ожован Михаил – Имперский колледж Лондона, Лондон, Великобритания

Попов Анатолий – Пенсильванский университет, Филадельфия, США

Статьи, поступившие в редакцию, рецензируются. За достоверность сведений, изложенных в статьях, ответственность несут авторы публикаций.

Мнение редакции может не совпадать с мнением авторов материалов.

Адрес редакции: 831 04, Словакия, г. Братислава,
Нове Место, ул. Стара Вайнорска, 1367/4

Дата выпуска 15.06.17.

Формат 21 × 29,7/4.

Сайт журнала: <http://ejournal14.com>
E-mail: evr2010@rambler.ru

Гарнитура Georgia.

Учредитель и издатель: Academic Publishing
House Researcher s.r.o.

Заказ № 110.

CONTENTS

Articles and Statements

Synthesis of 2,3-Disubstituted Quinazolinone Derivatives Using Silver Triflate as a Efficient Catalyst at Room Temperature M. Hari Krishna, P. Thriveni	4
Chemical Bath Deposition and Study of Semiconductor Thin Films in Cu ₂ S–In ₂ S ₃ System S.S. Tulenin, A.V. Pozdun, K.A. Karpov, D.A. Novotorkina, M.S. Rogovoi, L.N. Maskaeva, V.F. Markov	13
Theoretical Study of the Reactivity and Regioselectivity of the Addition Reaction between HCl and Alkenes, Investigation of the Markovnikov's Rule A. Zeroual, M.M. El Idrissi, M. Zoubir, A. Benharref	21
Theoretical Study of the Reactivity and Regioselectivity of the Addition Reaction between HCl and Alkenes, Investigation of the Markovnikov's Rule A. Zeroual, M.M. El idrissi, M. Zoubir, A. Benharref	28

Copyright © 2017 by Academic Publishing House Researcher s.r.o.



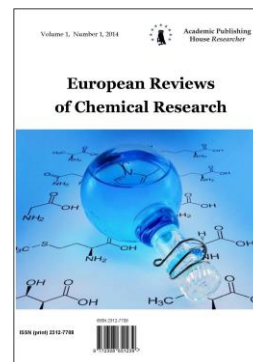
Published in the Slovak Republic
European Reviews of Chemical Research
Has been issued since 2014.

ISSN: 2312-7708

E-ISSN: 2413-7243

2017, 4(1): 4-12

DOI: 10.13187/erchr.2017.1.4

www.ejournal14.com

Articles and Statements

Synthesis of 2,3-Disubstituted Quinazolinone Derivatives Using Silver Triflate as a Efficient Catalyst at Room Temperature

M. Hari Krishna^a, P. Thriveni^{a,*}^a Department of Chemistry, Vikrama Simhapuri University, Nellore-524001, A.P., India

Abstract

Heterocyclic compounds are commonly used Scaffolds on which pharmacophores are arranged to provide potent and selective drugs. This is especially true for Nitrogen containing hetero cycles, which serve as the core components of many substances that possess a wide range of interesting biological activities. A series of 2,3-disubstituted quinazolinone derivatives have been synthesized in excellent yields at room temperature. The reaction was efficiently promoted by AgoTf. This protocol is very simple and provides moderate yields. All the products were identified by spectral (¹H NMR, ¹³C NMR and mass) and analytical data.

Keywords: synthesis, 2,3-disubstituted quinazolinone, silver triflate, room temperature.

1. Introduction

The chemistry of heterocyclic compounds represents half of all organic chemistry research worldwide. In particular, heterocyclic structures form the basis of many pharmaceutical and other bioactive products. Heterocyclic compounds form the basis of many pharmaceutical, agrochemical and veterinary products. Among a wide variety of nitrogen heterocyclic moieties that have been explored for developing pharmaceutically useful molecules, quinazolinone plays an important role in medicinal chemistry and subsequently have emerged as a pharmacophore that possess a diversity of useful biological activities. The pharmacodynamic versatility of quinazolin-4-one moiety has been documented not only in many of its synthetic derivatives but also in several naturally occurring alkaloids isolated from animals, plants and microorganisms.

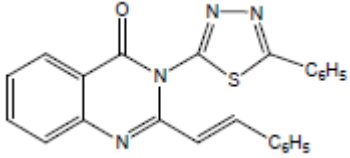
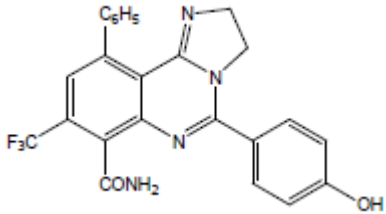
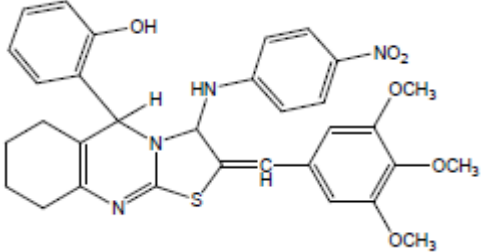
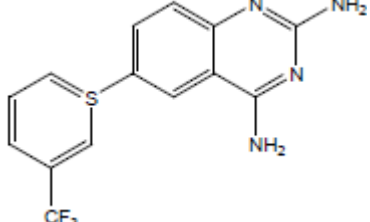
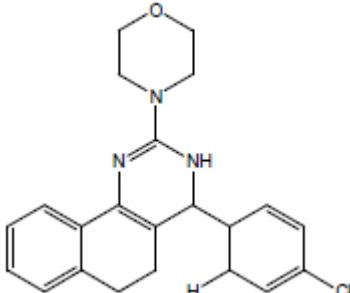
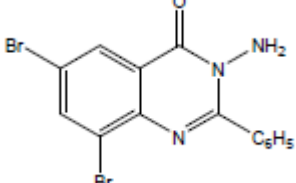
Literature survey revealed the versatile biological activities of quinazolinone derivatives (Büyüktimkin, 1985; Büyüktimkin et al., 1989). It has been established that quinazolinones possess antiviral (Mukherji et al., 1980), antifungal (Peet et al., 1986), antiallergic (Chaurasia, Sharma, 1982), antitumor (Li et al., 2012), antidiabetic activities (Chiou et al., 1996), coronary vasodilatory (Nagase et al., 2008), histamine receptor type-3 inverse agonism (Pandey, Lohani, 1979), anti cancer (Murugan et al., 2003; Shankar et al., 1984), anti-inflammatory (Shankar et al., 1985; Abdel-Aim's et al., 1994; Mohd, Shalini, 1998; Saravanan et al., 1998; Bhat et al., 2000) anti-tuberculosis (Kumar et al., 1970), CNS depressant activity (Tiwari, Pandey, 1975), anti-

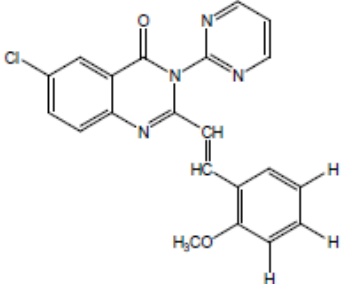
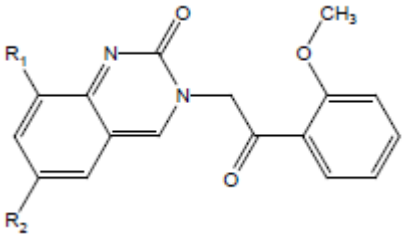
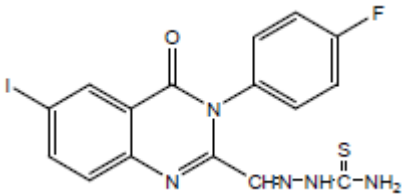
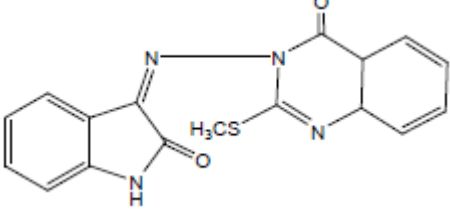
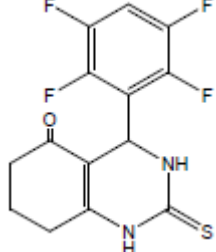
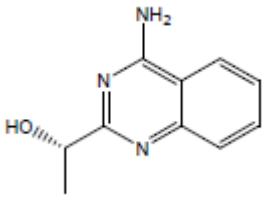
* Corresponding author

E-mail addresses: Thrivenivsu@gmail.com (P. Thriveni)

parkinsonism (Tiwardi, Rastogi, 1978; Srivastava et al., 1986) and bronchodilator activity (Rao, Bahekar, 1999).

Table 1. Some of Quinazolinone derivatives with their biological activities

	<p>3-(5-phenyl-1,3,4-thiadiazol-2-yl)-2-styrylquinazolin-4(3H)-one (CNS depressant activity)</p>
	<p>8-(trifluoromethyl)-2,3-dihydro-5-(4-hydroxyphenyl)-10-phenylimidazo[1,2-c]quinazoline-7-carboxamide (anti-inflammatory activity)</p>
	<p>2-(2-(3,4,5-trimethoxybenzylidene)-3-(4-nitrophenylamino)-3,5,6,7,8,9-hexahydro-2H-thiazolo[2,3-]quinazolin-5-yl)phenol (antioxidant activity)</p>
	<p>6-(3-(trifluoromethyl)thiopyran-1-yl)quinazoline-2,4-diamine (antimalarial activity)</p>
	<p>4-(4-chlorocyclohexa-2,4-dienyl)-3,4,5,6-tetrahydro-2-morpholino benzo[h]quinazoline (antileishmanial activity)</p>
	<p>6,8-dibromo-2-phenyl benzoxazines (analgesic activity)</p>

	<p>2-(2-methoxystyryl)-6-chloro-3-(pyrimidin-2-yl)quinazolin-4(3H)-One (antileukemic activity)</p>
	<p>3-(2-(2-methoxyphenyl)-2-oxoethyl)quinazolinone derivatives (anticoccidial activity)</p>
	<p>1-((3-(4-fluorophenyl)-3,4-dihydro-6-iodo-4-oxoquinazolin-2-yl)methylene)thiosemicarbazides (anticonvulsant activity)</p>
	<p>3-(2-oxoindolin-3-ylideneamino)-2-(methylthio)quinazolin-4(3H,4aH,8aH)-one (anti HIV activity)</p>
	<p>4-(2,3,5,6-tetrafluorophenyl)-1,2,3,4,7,8-hexahydro-2-thioxoquinazolin-5(6H)-one (antifungal activity)</p>
	<p>(S)-1-(4-Aminoquinazolin-2-yl)ethanol (animutagenic activity)</p>

In view of their importance, many approaches have been developed for the preparation of quinazolinone derivatives. Several methods for the synthesis of 4(3H)-quinazolinones have been investigated in the past. Some common methods include the condensation of 2-aminobenzamides and substituted benzoyl chlorides or their equivalents in ionic liquids (Potewar et al., 2005; Wang et al., 2012), the tandem condensation and C–N cross coupling of 2-halobenzoic acids and amidines (Zhang et al., 2009), the cyclization of o-acylaminobenzamides (Armarego, 1979), 2-aminobenzonitrile (Bogert, Hand, 1902), N-aryl orthanilamides (Stephen, Wadge, 1956; Segarra et al., 1998), nitroenes (Akazome, 1995), and aza-Wittig reactions of a-azido-substituted aromatic imides (Takeuchi et al., 1989; Takeuchi et al., 1991). However, benzyl chlorides are carcinogenic alkylating

agents and poisonous lachrymators and the base K_2CO_3 is needed to neutralize the hydrochloride produced during the reaction (Adib et al., 2011). Very recently, Ma developed a CuI–4-hydroxy-L-proline catalyzed coupling involving N-substituted o-bromobenzamides and formamide or other amides to afford 3-substituted quinazolinones directly, or 2,3-disubstituted quinazolinones via a HMDS– $ZnCl_2$ mediated condensative cyclization (Xu et al., 2012). Unfortunately, both approaches lead to the generation of undesired byproducts, such as hydrogen halide which consumes K_2CO_3 making the overall process less efficient in terms of atom economy. Dabiri et al. reported a one-pot three-component route to synthesize 2,3-disubstituted 4(3H)-quinazolinones in the presence of an equivalent amount of iodine as the catalyst (Dabiri et al., 2010). Recently, a series of Quinazolinone derivatives were synthesised from isatoic anhydride and benzimidamide using BBr_3 as a catalyst (Yedukondalu et al., 2017), and Tandem cyclization of 2-halobenzoic acids with amidines using Cerium(III) chloride as catalyst (Yedukondalu et al., 2017), one-pot reaction using a three-component condensation of anthranilic acid, amines, and ortho esters at room temperature under solvent-free conditions (Hari Krishna, Thriveni, 2017). Recently, transition-metal-catalyzed reactions have emerged as versatile tools for the construction of quinazolinones. For example, palladium-catalyzed carbonylation/cyclization cascades turned out to be an efficient approach toward quinazolinone derivatives (He et al., 2014; Wu et al., 2013). However, most of these procedures have some drawbacks, as they have a poor atom economy, use expensive chemicals. Therefore, the development of more practical and efficient approaches toward quinazolinone derivatives remains an attractive task for organic chemists. Herein we report an efficient synthesis of 4(3H)-quinazolinones using Silver triflate (10 mol%) as catalyst (Scheme I).

2. Materials and methods

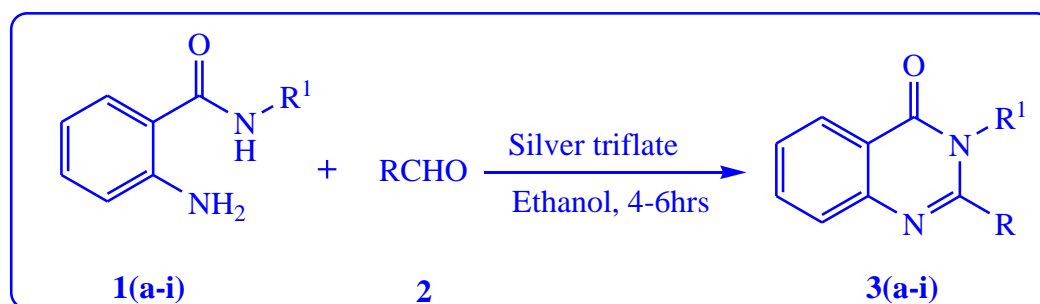
Compounds were checked for their purity by TLC on silica gel G plates and spots were located by iodine vapours. The NMR spectra were measured with a 400 MHz Bruker Avance spectrometer at 400.1 and 100.6 MHz and spectra (1H NMR and ^{13}C NMR) were recorded using tetramethylsilane (TMS) in the solvent of $CDCl_3-d$ or $DMSO-d_6$ as the internal standard (1H NMR: TMS at 0.00 ppm, $CDCl_3$ at 7.26 ppm, DMSO at 2.50 ppm. ^{13}C NMR: $CDCl_3$ at 77.16 ppm, DMSO at 40.00 ppm).

General Procedure for the synthesis of 2,3-diSubstituted Quinazolinone derivatives 3(a-i):

The catalyst Silver triflate (10 mol %) was added to a mixture of 2-aminobenzamide (2 mmol) in ethanol and aldehyde (3 mmol) at room temperature under N_2 and the reaction mixture stirred for 4-6hrs. The progress of the reaction was monitored by TLC. After completion, the system was cooled to room temperature. The reaction mixture was diluted with water (15 ml), filter and dried over Na_2SO_4 and concentrated under reduced pressure to give the crude product. The crude compound was purified through the silica gel column chromatography using ethyl acetate and hexane (30:70) as eluent affords the product in 75-88 % yield. All the products were identified by spectral (1H NMR, ^{13}C NMR and mass) and analytical data

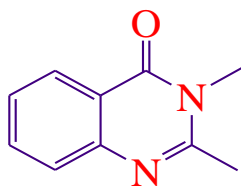
Scheme I: The synthetic route was depicted in Scheme I.

Scheme 1



synthesis of 2,3-disubstituted 4(3H)-quinazolinones

Spectral data for selected compounds:

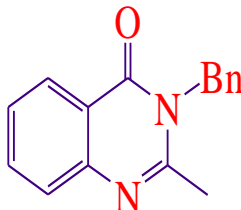
2,3-dimethylquinazolin-4(3H)-one (3a):

White solid, mp 110-111°C;

¹H NMR (CDCl₃, 400 MHz): δ 2.63 (s, 3H), 3.62 (s, 3H), 7.44 (dt, *J*₁ = 8.0 Hz, *J*₂ = 1.2 Hz, 1H), 7.61 (d, *J* = 8.0 Hz, 1H), 7.71 (dt, *J*₁ = 8.0 Hz, *J*₂ = 1.2 Hz, 1H), 8.25 (dd, *J*₁ = 8.0 Hz, *J*₂ = 1.2 Hz, 1H) ppm;

¹³C NMR (CDCl₃, 100 MHz): δ 23.6, 31.1, 120.2, 126.5, 126.5, 126.8, 134.3, 147.1, 154.6, 162.3, ppm;

HRMS (ESI): *m/z* [M+H]⁺ calcd. for C₁₀H₁₀N₂O 175.0866; found 175.0870.

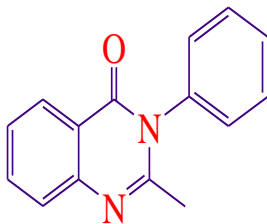
3-benzyl-2-(4-oxopentyl)quinazolin-4(3H)-one (3b):

Pale yellow solid, mp 122-124°C;

¹H NMR (CDCl₃, 400 MHz): δ = 2.04-2.08 (m, 2H), 2.11 (s, 3H), 2.56 (t, *J* = 6.8 Hz, 2H), 2.74 (t, *J* = 7.6 Hz, 2H), 5.49 (s, 2H), 7.19 (d, *J* = 6.8 Hz, 2H), 7.27-7.36 (m, 3H), 7.47 (dt, *J*₁ = 8.0 Hz, *J*₂ = 0.8 Hz, 1H), 7.65 (d, *J* = 8.0 Hz, 1H), 7.75 (dt, *J*₁ = 8.4 Hz, *J*₂ = 1.6 Hz, 1H), 8.32 (dd, *J*₁ = 8.0 Hz, *J*₂ = 1.2 Hz, 1H);

¹³C NMR (CDCl₃, 100 MHz): δ = 20.9, 30.1, 34.1, 42.3, 46.3, 120.4, 126.4, 126.6, 127.0, 127.2, 127.6, 128.9, 134.4, 136.3, 147.2, 156.6, 162.6, 208.3;

HRMS (ESI): *m/z* [M+H]⁺ calcd. for C₂₀H₂₀N₂O₂ 321.1598; found 321.1605.

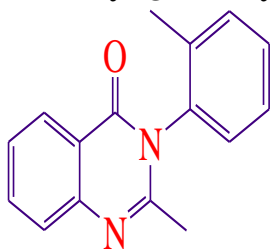
2-methyl-3-phenylquinazolin-4(3H)-one (3c):

White solid, mp 147-148°C;

¹H NMR (CDCl₃, 400 MHz): δ = 2.25 (s, 3H), 7.27-7.28 (m, 2H), 7.46-7.59 (m, 4H), 7.68 (d, *J* = 7.6 Hz, 1H), 7.77 (dt, *J*₁ = 8.4 Hz, *J*₂ = 1.6 Hz, 1H), 8.28 (dd, *J*₁ = 8.0 Hz, *J*₂ = 1.2 Hz, 1H);

¹³C NMR (CDCl₃, 100 MHz): δ 24.4, 120.8, 126.7, 126.8, 127.1, 128.0, 129.3, 130.0, 134.6, 137.8, 147.5, 154.2, 162.3;

HRMS (ESI): *m/z* [M+H]⁺ calcd. for C₁₅H₁₂N₂O 237.1022; found 237.1028.

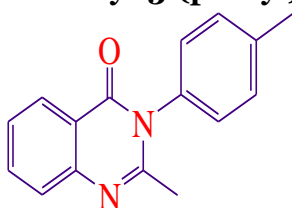
2-methyl-3-(*o*-tolyl)quinazolin-4(3*H*)-one (3d):

White solid, mp 119-121°C;

¹H NMR (CDCl₃, 400 MHz): δ = 2.13 (s, 3H), 2.19 (s, 3H), 7.16 (d, *J* = 7.6 Hz, 1H), 7.35-7.42 (m, 3H), 7.48 (t, *J* = 7.6 Hz, 1H), 7.69 (d, *J* = 8.0 Hz, 1H), 7.78 (dt, *J*₁ = 8.4 Hz, *J*₂ = 1.2 Hz, 1H), 8.29 (dd, *J*₁ = 8.0 Hz, *J*₂ = 0.8 Hz, 1H);

¹³C NMR (CDCl₃, 100 MHz): δ = 17.4, 23.9, 120.7, 126.6, 126.9, 127.1, 127.6, 127.9, 129.6, 131.5, 134.6, 135.3, 136.8, 147.6, 154.3, 161.7;

HRMS (ESI): *m/z* [M+H]⁺ calcd. for C₁₆H₁₄N₂O 251.1179; found 251.1186.

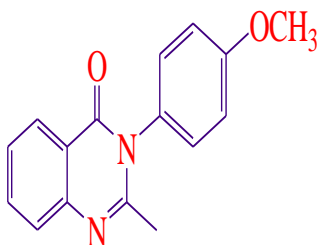
2-methyl-3-(*p*-tolyl)quinazolin-4(3*H*)-one (3e):

White solid, mp 150-151°C;

¹H NMR (CDCl₃, 400 MHz): δ = 2.25 (s, 3H), 2.45 (s, 3H), 7.14 (d, *J* = 8.0 Hz, 2H), 7.35 (d, *J* = 7.6 Hz, 2H), 7.46 (t, *J* = 7.6 Hz, 1H), 7.67 (d, *J* = 8.4 Hz, 1H), 7.76 (dt, *J*₁ = 8.0 Hz, *J*₂ = 0.8 Hz, 1H), 8.26 (d, *J* = 8.0 Hz, 1H) ppm;

¹³C NMR (CDCl₃, 100 MHz): δ = 21.3, 24.4, 120.8, 126.5, 126.7, 127.1, 127.7, 130.6, 134.5, 135.1, 139.3, 147.5, 154.5, 162.4;

HRMS (ESI): *m/z* [M+H]⁺ calcd. for C₁₆H₁₄N₂O 251.1179; found 251.1185.

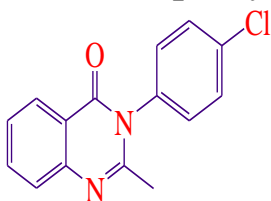
3-(4-methoxyphenyl)-2-methylquinazolin-4(3*H*)-one (3f):

White solid, mp 169-171°C;

¹H NMR (CDCl₃, 400 MHz): δ = 2.26 (s, 3H), 3.88 (s, 3H), 7.05 (d, *J* = 8.8 Hz, 2H), 7.17 (d, *J* = 8.8 Hz, 2H), 7.46 (t, *J* = 7.6 Hz, 1H), 7.67 (d, *J* = 8.0 Hz, 1H), 7.76 (dt, *J*₁ = 8.4 Hz, *J*₂ = 1.2 Hz, 1H), 8.26 (dd, *J*₁ = 8.0 Hz, *J*₂ = 0.8 Hz, 1H);

¹³C NMR (CDCl₃, 100 MHz): δ = 24.4, 55.5, 115.2, 120.8, 126.6, 126.7, 127.1, 129.0, 130.2, 134.5, 147.5, 154.9, 159.9, 162.5;

HRMS (ESI): *m/z* [M+H]⁺ calcd. for C₁₆H₁₄N₂O₂ 267.1128; found 267.1135.

3-(4-chlorophenyl)-2-methylquinazolin-4(3*H*)-one (3g):

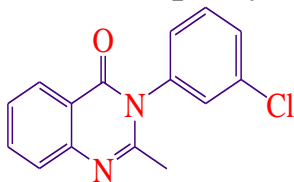
White solid, mp 157-158°C;

¹H NMR (CDCl₃, 400 MHz): δ = 2.25 (s, 3H), 7.22 (d, *J* = 8.4 Hz, 2H), 7.48 (t, *d* = 8.4 Hz, 1H), 7.54 (d, *J* = 8.4 Hz, 2H), 7.68 (d, *J* = 8.0 Hz, 1H), 7.78 (t, *J* = 7.2 Hz, 1H), 8.26 (d, *J* = 8.0 Hz, 1H);

¹³C NMR (CDCl₃, 100 MHz): δ = 24.4, 120.6, 126.8, 127.1, 129.6, 130.3, 134.8, 135.4, 136.2, 147.4, 153.7, 162.2;

HRMS (ESI): *m/z* [M+H]⁺ calcd. for C₁₅H₁₁ClN₂O 271.0633; found 271.0639.

3-(3-chlorophenyl)-2-methylquinazolin-4(3*H*)-one (3h):



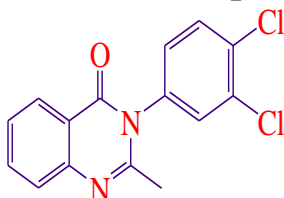
White solid, mp 130-131°C;

¹H NMR (CDCl₃, 400 MHz): δ = 2.27 (s, 3H), 7.18-7.21 (m, 1H), 7.31 (s, 1H), 7.46-7.51 (m, 3H), 7.68 (d, *J* = 8.4 Hz, 1H), 7.79 (dt, *J*₁ = 8.0 Hz, *J*₂ = 1.2 Hz, 1H), 8.26 (dd, *J*₁ = 8.0 Hz, *J*₂ = 0.8 Hz, 1H);

¹³C NMR (CDCl₃, 100 MHz): δ = 24.4, 120.6, 126.6, 126.9, 126.9, 127.1, 128.6, 129.7, 131.0, 134.8, 135.6, 138.8, 147.4, 153.5, 162.1;

HRMS (ESI): *m/z* [M+H]⁺ calcd. for C₁₅H₁₁ClN₂O 271.0633; found 271.0641.

3-(3,4-dichlorophenyl)-2-methylquinazolin-4(3*H*)-one (3i):



White solid, mp 164-165°C;

¹H NMR (CDCl₃, 400 MHz): δ = 2.26 (s, 3H), 7.13 (d, *J* = 8.8 Hz, 1H), 7.41 (s, 1H), 7.46 (t, *J* = 7.2 Hz, 1H), 7.61-7.68 (m, 2H), 7.77 (t, *J* = 7.6 Hz, 1H), 8.21 (d, *J* = 7.6 Hz, 1H) ppm;

¹³C NMR (CDCl₃, 100 MHz): δ = 24.3, 120.2, 126.9, 126.9, 126.9, 127.6, 130.2, 131.6, 133.9, 134.0, 134.9, 136.8, 147.2, 153.1, 161.9 ppm;

HRMS (ESI): *m/z* [M+H]⁺ calcd. for C₁₅H₁₀Cl₂N₂O 305.0243; found 305.0252.

4. Results and discussion

In our preliminary investigation on the model reaction of 2-aminobenzamide and aldehyde, it was found that the reaction could be finished under very simple reaction conditions in the presence of Silver triflate as catalyst which gives the desired Quinazolinone product in good yield

2-aminobenzamide **1** with aldehyde **2** in the presence of Silver triflate catalyst proceeded rapidly in ethanol solvent at room temperature to afford 2,3-disubstituted Quinazolinone (Scheme I). Any excess of Silver triflate (10 mol%) beyond this loading did not show any substantial improvement in the yield. So 10 mol% of Silver triflate chosen as the optimal loading of the catalyst. The reaction was carried out at room temperature. The results indicated that a wide range of structurally varied 2-aminobenzamide reacted smoothly to give the Quinazolinone in good yields (scheme 1). Readily available starting materials and simple synthesizing procedures make this method very attractive and convenient for the synthesis of 2,3-disubstituted Quinazolinone derivatives. Formation of products was confirmed by recording their ¹H NMR, ¹³C, mass spectra.

5. Conclusion

In conclusion we have developed a simple methodology for the preparation of 2,3-disubstituted Quinazolinone derivatives by using Silver triflate (10 mol%) as efficient catalyst. The notable features of this procedure are mild reaction conditions, good yield, enhanced rates and simplicity in operation, which make it a useful and attractive process for the synthesis of 2,3-disubstituted quinazolinone derivatives. Thus, the developed methodology could be an alternative for the academic as well as industrial applications.

6. Acknowledgement

Authors are thankful to our Research Supervisor Dr. P. Thriveni for providing us required facilities and motivation for completion of the research work. We also extend our gratitude towards BRNS, BARC, Mumbai for financial assistance and IICT, Hyderabad for providing us facilities of IR Spectra, ¹H NMR for characterization of synthesized compounds.

References

- Büyüktimkin, 1985 – Büyüktimkin S. (1985). *Arch Pharm.* 318, 496–501.
- Büyüktimkin et al., 1989 – Büyüktimkin S, Büyüktimkin N, Özdemir O. (1989). *Arch Pharm.* 322, 49–52.
- Mukherji et al., 1980 – Mukherji DD, Nintiyal SR, Prasad CR, Dhawan BN. (1980). *Ind J Med Res.* 93, 1426–1432.
- Peet et al., 1986 – Peet NP, Baugh LE, Sunder S. (1986). *J Med Chem.* 29, 2403–2409.
- Chaurasia, Sharma, 1982 – Chaurasia MR, Sharma SK. (1982). *Arch Pharm.* 315, 377–381.
- Li et al., 2012 – Li H, Wang JP, Yang F. (2012). *Heterocycles.* 85, 1897–1911.
- Chiou et al., 1996 – Chiou WF, Liao JF, Chen CF. (1996). *J Nat Prod.* 59, 374–378.
- Nagase et al., 2008 – Nagase T, Mizutani T, Ishikawa S. (2008). *J Med Chem.* 51, 4780–4789.
- Pandey, Lohani, 1979 – Pandey V.K., Lohani H.C. (1979). *J Indian Chem. Soc.* 56, 415.
- Murugan et al., 2003 – Murugan V., Padmavaty N.P., Ramasarma G.V.S. *I.J.H.C.* 13, 143.
- Shankar et al., 1984 – Ravi Shankar, Ch, Devender Rao, A, MallaReddy V & Sattur P.B. (1984). *Curr. Sci.* 53, 1069.
- Shankar et al., 1985 – Ravi Shankar Ch, Devender Rao. A, MallaReddy V. (1985). *Indian Drugs*, 24B, 580.
- Abdel-Aim's et al., 1994 – Abdel-Aim's, Abdel-Nasser A, Shorbagi, Hosny A.H. (1994). *Indian J. Chem.* 33B, 260.
- Mohd, Shalini, 1998 – Mohd. Amir, Shalini Shahani (1998). *Indian J. Heterocycl. Chem.* 8,107.
- Saravanan et al., 1998 – Saravanan, S. Mohan, K.S. Manjunatha (1998). *I.J.H.C.* 8, 55.
- Bhat et al., 2000 – A.R. Bhat, G. Goutham Shenoy, Mohan Kotian (2000). *Indian J. Heterocycl, Chem.* 9, 319.
- Kumar et al., 1970 – R. Kumar, T.K. Gupta, Surendra S. Parmar (1970). *Indian J. Pharm.* 33, 108.
- Tiwari, Pandey, 1975 – Tiwari SS, Pandey VK. (1975). *J. Indian Chem. Soc.* 52, 736.
- Tiwardi, Rastogi, 1978 – S.Tiwardi SS, Rastogi RK (1978). *J Indian Chem. Soc.* 55, 477.
- Srivastava et al., 1986 – Vijay K. Srivastava, I.P. Singh, ShrodhaSingh M.B. Gupta, K. Shanker (1986). *Indian J Pharm. Sci.* 48, 133.
- Rao, Bahekar, 1999 – A. Raghu Ram Rao, Rajesh H Bahekar (1999). *I.J.C.*, 38B, 434.
- Potewar et al., 2005 – T. M. Potewar, R. N. Nadaf, T. Daniel, R. J. Lahoti, K. V. Srinivasan (2005). *Synth. Commun.* 35, 231–241.
- Wang et al., 2012 – S. L. Wang, K. Yang, C. S. Yao, X. S. Wang (2012). *Synth. Commun.* 42, 341–349.
- Zhang et al., 2009 – X. Zhang, D. Ye, H. Sun, D. Guo, J. Wang, H. Huang, X. Zhang, H. Jiang, H. Liu (2009). *Green Chem.* 11, 1881–1888.
- Armarego, 1979 – W. L. F. Armarego (1979). *Adv. Heterocycl. Chem.* 24, 1–62.
- Bogert, Hand, 1902 – M. T. Bogert, W. F. Hand (1902). *J. Am. Chem. Soc.* 24, 1031–1050.
- Stephen, Wadge, 1956 – H. Stephen, G. Wadge (1956). *J. Chem. Soc.* 4420–4421.
- Segarra et al., 1998 – Segarra V. Segarra, M. I. Crespo, F. Pujol, J. Belata, T. Domenech, M. Miralpeix, J. M. Palacios, A. Castro, A. Martinez (1998). *Bioorg. Med. Chem. Lett.*, 8, 505–510.
- Akazome, 1995 – M. Akazome, J. Yamamoto, T. Kondo, Y. Watanabe (1995). *J. Organomet. Chem.*, 494, 229–233.
- Takeuchi et al., 1989 – H. Takeuchi, S. Haguvara, S. Eguchi (1989). *Tetrahedron*, 45, 6375–6386.
- Takeuchi et al., 1991 – H. Takeuchi, S. Haguvara, S. Eguchi (1991). *J. Org. Chem.* 56, 1535–1537.
- Adib et al., 2011 – M. Adib, E. Sheikhi, H. R. Bijanzadeh (2011). *Synlett*, 2012, 85–88.

Xu et al., 2012 – L. Xu, Y. Jiang, D. Ma (2012). *Org. Lett.* 14, 1150–1153.

Dabiri et al., 2010 – M. Dabiri, P. Salehi, M. Bahramnejad, M. Alizadeh (2010). *Monatsh. Chem.* 141, 877–881.

Yedukondalu et al., 2017 – B. Yedukondalu, B. Lalitha kumari, M. Hari Krishna, P. Thriveni (2017). *Heterocyclic letters*, 7 (1), 91-97.

Yedukondalu et al., 2017 – B. Yedukondalu, B. Lalitha kumari, M. Hari Krishna, P. Thriveni (2017). *Heterocyclic letters*, 7 (1), 141-146.

Hari Krishna, P. Thriveni, 2017 – M. Hari Krishna, P. Thriveni (2017). *Heterocyclic letters*, 7(1), 113-120.

He et al., 2014 – L. He, H. Li, H. Neumann, M. Beller, X.-F. Wu (2014). *Angew. Chem., Int. Ed.*, 53, 1420.

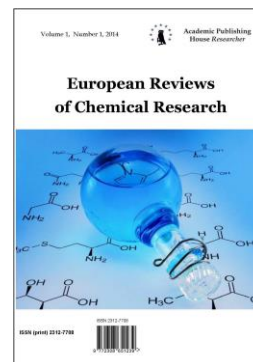
Wu et al., 2013 – X.-F. Wu, L. He, H. Neumann, M. (2013). *Beller, Chem.–Eur. J.*, 19, 12635.

Copyright © 2017 by Academic Publishing House Researcher s.r.o.



Published in the Slovak Republic
European Reviews of Chemical Research
Has been issued since 2014.
ISSN: 2312-7708
E-ISSN: 2413-7243
2017, 4(1): 13-20

DOI: 10.13187/erchr.2017.1.13
www.ejournal14.com



Chemical Bath Deposition and Study of Semiconductor Thin Films in $\text{Cu}_2\text{S}-\text{In}_2\text{S}_3$ System

Stanislav S. Tulenin^a, Andrei V. Pozdun^a, Konstantin A. Karpov^a, Darya A. Novotorkina^a, Michael S. Rogovoi^a, Larisa N. Maskaeva^a, Vyacheslav F. Markov^{a,*}

^a Ural Federal University named after the first President of Russia B.N. Yeltsin, Ekaterinburg, Russian Federation

Abstract

In the first time thin films of $\text{In}_x\text{Cu}_{1-x}\text{S}_y\text{O}_{1-y}$ composition with the content of indium up to 9.63 at% were obtained by means of a chemical bath deposition from a system “indium chloride – copper chloride – sodium hydroxide – thiourea” and “indium chloride – copper chloride – sodium hydroxide – trilon B – thiourea”. The experimental data on the distribution and the atomic ration of elements in synthesized patterns obtained by the x-ray photoelectron spectroscopy were discussed. The change in the surface microstructure of thin films depending on the temperature and the composition of reaction bath were determined by means of scanning electron microscopy. The structure of obtained thin films has *n*-type of conductivity.

Keywords: copper sulfide (I), indium sulfide(III), thin films, solid solutions of replacement, x-ray photoelectron spectroscopy.

1. Introduction

The people stands near to a new discover that connected with solution of difficult problems. As last decades a great force was direct to solution of removable energy problem. The scientific attention in any removable field direct to a new semiconductor material and this deposition method. The thin film chalcopyrite structures we can refer to promising material for solar cells.

The first representative in a line of chalcopyrite semiconductor is copper(I)-indium(III) disulfide $\text{Cu}_2\text{S}-\text{In}_2\text{S}_3$. Collection of a properties such as high absorption factor of incident sunlight α ($\sim 10^{-5} \text{ cm}^{-1}$) (Jing-Jing et al., 2012), optimal energy band gap (1.5 eV) (Novoselova, 1979), rather high efficiency factor ($\sim 13\%$) (Fiechter, 2008), radiation stability (Maier et al., 2011), low industrial cost and environment safety in comparison with CdS is causing that these semiconductors use for solar cells preparation. Moreover a improvement of optical properties of chalcopyrite thin films $\text{Cu}_2\text{S}-\text{In}_2\text{S}_3$ is caring out by means of control doping by elements such as Ga, Zn, Fe, Se doping (Yanfeng et al., 2011; Kuan-ting et al., 2013; Sharma et al., 2009).

There are different deposition methods for semiconductor material in a system $\text{Cu}_2\text{S}-\text{In}_2\text{S}_3$. For example, it is high-speed magnetron spraying in a vacuum, spraying of water solutions with pyrolysis on heating a substrate (Lee, JunHo, 2010), physical deposition from gas phase, molecular-beam epitaxy (Chepra, Das, 1986), deposition by a sulfidization method on separate

* Corresponding author

E-mail addresses: dkgoran.rajovic@gmail.com (V.F. Markov)

layers Cu-In (Merdes et al., 2011), electrochemical deposition (Jing-Jing et al., 2012) and chemical bath deposition (CBD) (Sharma et al., 2009; Yoon et al., 2012).

Attractiveness of CBD is not only its technology simplicity, the absence of deep vacuum or high temperature but also a deposition possibility for supersaturated solid solution, flexible control of a film properties that is vary difficult or impossible to achieve. As a result these factors are promising a low-temperature chemical deposition methods for copper(I)-indium(III) disulfide. However, literature data about complex physical and chemical studies for thin films of copper (I) and indium (III) sulfides and this replaced solid solution by CBD is absent.

Earlier we noticed from carried out thermodynamic researches (Fedorova et al., 2015; Maskaeva et al., 2012) that is a concentration region for copper (I) and indium (III) sulfides codeposition in two different system: hydroxide-system and trilonate-system. Also we showed that is a wide region of indium hydroxide steady which can impede a sulfide phase formation.

Purpose of the present work is carrying out of chemical bath co-deposition of thin films of copper (I) and indium sulfides and physical and chemical studies of their composition and microstructure.

2. Materials and methods

Deposition of Cu(I)-In-S thin films was carrying out on preliminary defatting sitall substrates (CT-50-1 mark) from two different reaction mixture. The first of them contained indium chloride InCl_3 , copper chloride CuCl_2 , sodium hydroxide NaOH , thiourea $\text{N}_2\text{H}_4\text{CS}$. The second reaction mixture additionally contained trilon B $\text{Na}_2\text{C}_{10}\text{H}_{14}\text{O}_8\text{N}_2 \cdot 2\text{H}_2\text{O}$. The $\text{NH}_2\text{OH} \cdot \text{HCl}$ addition in reaction mixture had entered to transfer the copper Cu^{2+} in Cu^+ . The synthesis of thin films was carried out in a range of temperatures 333–353 K in glass leak proof reactors in which substrates fixed in specially made ftoroplaste device were placed. Reactors were located in thermostat TC-TB-10 with the accuracy of maintenance of temperature $\pm 0.1^\circ$. Deposition time 120 minutes was fixed for all thin films. Thickness of obtained simples has been measured on interferometer Linnik's MII-4M. Dark resistance measurements of semiconductor Cu(I)-In-S thin films has been measured on equipment K.54.410. Composition and main form of compounds in thin films were studied by means of X-ray photoelectron spectroscopy (XPS) method on ESCALAB MK II (VG Scientific, Great Britain) X-ray photoelectron spectrometer using magnesium cathode $\text{MgK}\alpha$ (1253.6 eV) as the non-monochromatized X-ray excitation source. The $\text{Cu}2p_{5/2}$ line was calibration line with energy 932.5 eV. Scanning electron microscopy (SEM) of a simple surface was occurred on JEOL JSM-6390 LA instrument in second electron (SE) with JED 2300 tool for energy dispersive X-ray (EDX) analysis. Semiconductor type of obtained thin films was studied by means of a generated voltage measures.

3. Results and discussions

Concentration region and codeposition pH for copper (I) and indium sulfides was obtained by predicted calculation of CBD condition in $\text{Cu}_2\text{S-In}_2\text{S}_3$ system. For this aim analyses of ion balances in two complex systems was carried out (Maskaeva et al., 2012) that revealed which copper (I) and indium sulfides co-deposition is possible in wide pH region from 3.5 to 10, but in the case of trilon B is the only possible in a high alkaline condition.

Smooth Cu-In-S thin films with rather good adhesion to sitall substrate were deposited in experiment from carried out thermodynamic researches. Colour of thin films changes from light-brown (send-coloured) up to dark-brown with green shade.

The study of a main element forms and them composition in Cu-In-S thin films were carried out by means of XPS. For this survey spectra, region $\text{In}3d$ electron core level of indium, region $\text{Cu}2p$ electron core level of copper, region $\text{S}2p$ electron core level of sulfur and region from 10 to 90 eV containing $\text{In}4d$ and $\text{Cu}3p$ peaks were recorded.

The XPS data showed that chalcopyrite thin film content indium from 4.05 to 9.63 at% with deposition condition and initial reagent concentrations (see table). The copper amount exceed indium and fluctuate from 25.76 to 49.43 at%, and sulfur is in deficiency (12.99–26.28 at%). High oxygen quantity, except for main elements, from 20.14 to 52.36 at% in studied films was obtained.

Table

Simple	In, at%	Cu, at%	S, at%	O, at%	[Trilon], M	T, K
1	8.89	25.76	12.99	52.36	–	343
2	4.15	49.43	26.28	20.14	–	353
3	4.05	47.08	20.74	28.13	0.03	343
4	9.63	40.65	18.46	31.26	0.03	353
CuInS ₂ (monocr.)	25.00	25.00	50.00	–		

We suggest that oxygen is being included in the different oxygen-keeping impurities such as Cu₂O, In(OH)₃, In₂O₃ entering into Cu₂S-In₂S₃ thin film composition at chemical deposition process. The formation of these metal sulfides in reaction deposition mixtures was confirmed by ionic balances calculation in (Maskaeva et al., 2012).

The chemical condition of elements in thin film surface layers was being determined by the position of In3*d*, Cu3*p*, S2*p* and O1*s* peak of electron core levels spectra of In, Cu, S and O atoms accordingly.

The In4*d* peak indicates a present of indium in deposited films. It consists of two components: the first with energy ~18.53 eV (fig. 1a), how we suggesting, is an indium oxide form, and the second with energy ~19.6 eV refer to sulfide form. The In3*d* electron core level with energy ~444.75 eV is more informative line. One a few deviate to high energy compared to standard peak energy 444.45 eV for indium sulfide. All over indicate that indium particularly remains in an oxide or hydroxide phase in Cu-In-S surface layers.

Spectral analyses revealed that a main chemical form of sulfur in Cu-In-S surface layers is copper (I) sulfide (fig. 1b). Thus a bounding energy ~161.48 eV for S2*p* electron core levels spectra of sulfur in all over cases was interpreted as formation of the copper (I) sulfide solid phase. It compare to creating of a good conditions in the reaction bath for Cu₂S formation that possible activates a sulfidization process of indium hydroxide and Cu-In-S thin film deposition. Present of the some peak with deviation to high energy show that sulfur has positive charge and enter to composition of a sulfates or sulfites.

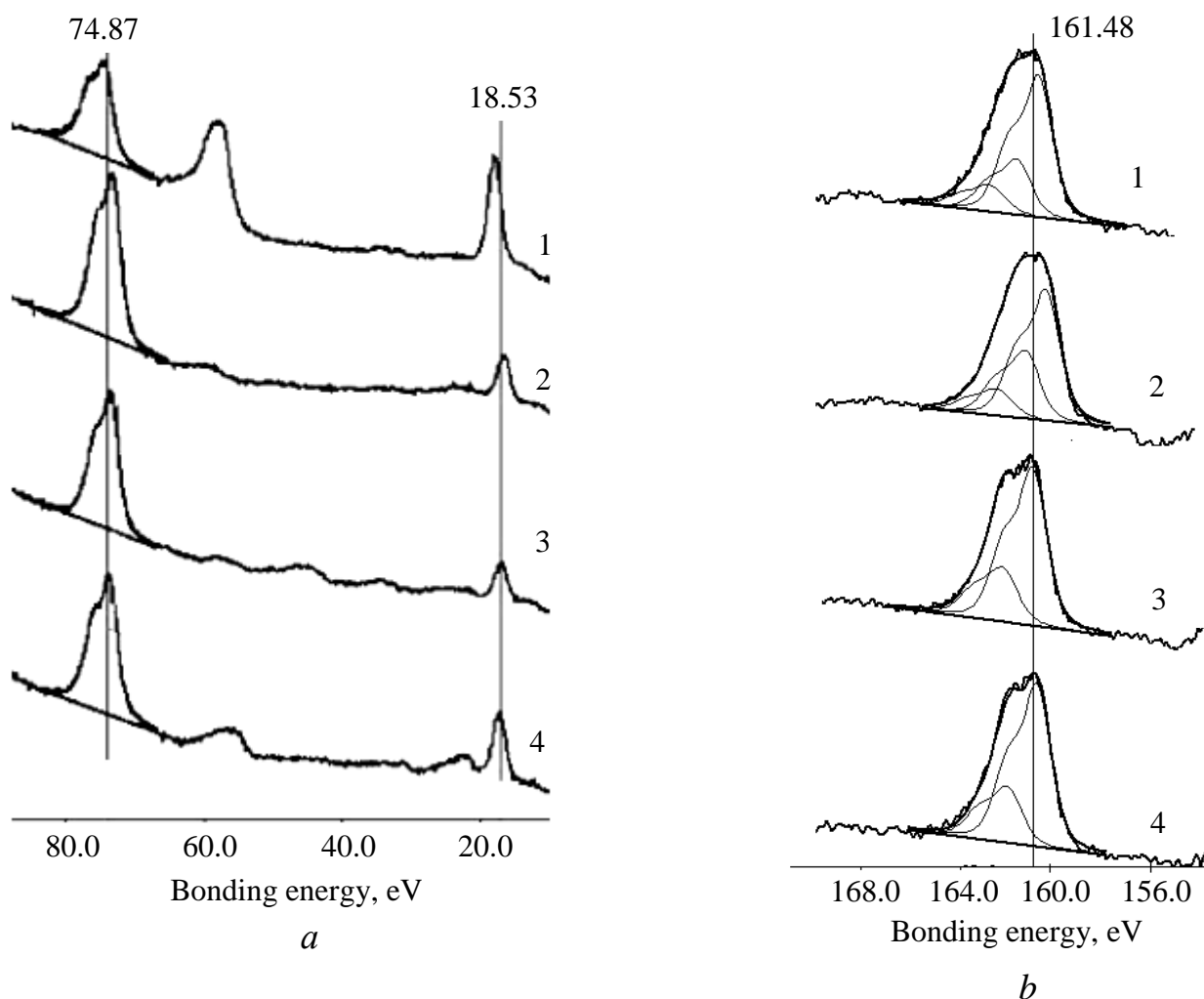


Fig. 1. XPS spectra of the samples: Cu_{3p}, In_{4d} (a) и S_{2p} (b) electron core levels spectra of copper, indium and sulfur in Cu₂S–In₂S₃ films. The photoelectron registration angle is 90° (analysis depth for layer is 2-4 nm)

XPS spectra of Cu_{2p} electron core level of deposited thin films with bonding energy 932.5 eV. On obtained spectra we clearly see that copper in layers fully is Cu⁺ due to hydroxide amine hydrochloride addition in reaction mixture. Apparently from [fig. 2](#) oxygen in films exist in two forms: oxide or hydroxide. There are peak with small bonding energy ~531.37 eV and peak with high bonding energy that refer to different organic, sulfate and sulfite impurities said about it. From XPS data we can conclude that the compound In_xCu_{1-x}S_yO_{1-y} with complex composition is formed in surface layers.

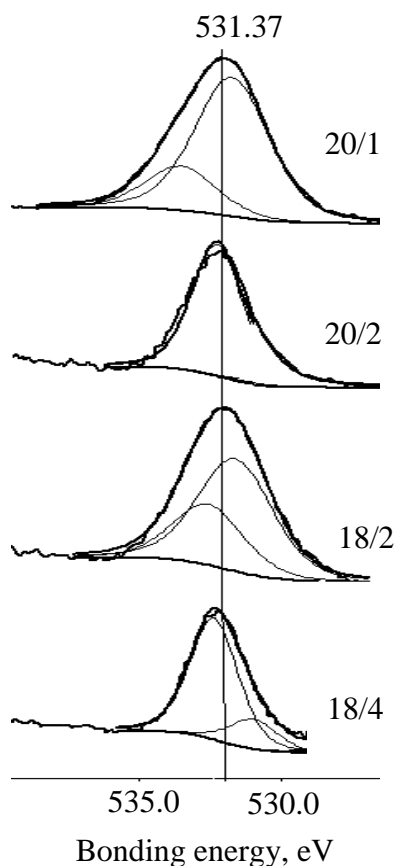


Fig. 2. XPS spectra of the samples: Cu2p (a) и O1s (b) electron core levels spectra of copper and oxygen in Cu-In-S

The SEM study of a deposited Cu_2S thin film structure (fig. 3) showed that it consists of sickle-like particles which don't have accurate crystallographic facet with size 110–500 nm. We can see small spherical agglomerates on surface with the same composition as main layer.

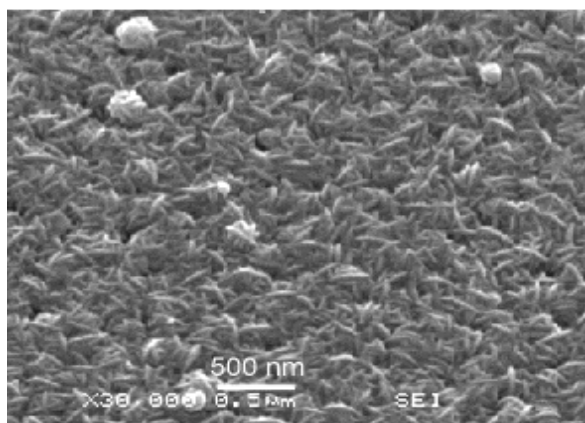


Fig. 3. SEM microphotograph of the make-up deposited Cu_2S film in second electron (magnification 30000)

The SEM data showed that addition of indium salt in reaction mixture is leading to decrease in particle size up to 76–230 nm (fig. 4) and formation of aggregates not possessing express habitus.

This is formation of $\text{In}_x\text{Cu}_{1-x}\text{S}_y\text{O}_{1-y}$ thin films from particles with average size 100–230 nm due to increase CBD temperature. Morphology don't have visual transformation due to increase

temperature up to 353 K (fig. 4c), but pellet size non-uniformity simultaneous increase.

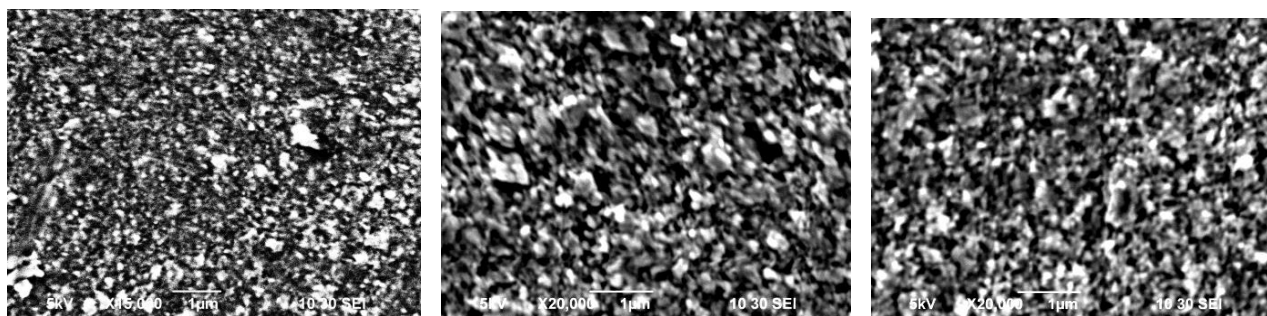


Fig. 4. SEM of the make-up deposited $\text{In}_x\text{Cu}_{1-x}\text{S}_y\text{O}_{1-y}$ film from reaction mixture including copper chloride, indium chloride, sodium hydroxide, hydroxide amine hydrochloride and thiourea, at temperature, K: 333 (a), 343 (b) и 353 (c)

We notice that a measured film $\text{In}_x\text{Cu}_{1-x}\text{S}_y\text{O}_{1-y}$ thickness by interferential microscope (Linnik's interferometer) depend on temperature at 333–353 K and increase from 320 to 570 nm. Reaction mixture, in it case, consists of copper chloride, indium chloride, sodium hydroxide, hydroxide amine hydrochloride and thiourea.

The complexing agents to inhibit extraction of copper in the precipitate in considered system in a number with copper hydroxides CuOH ($pK_{\text{H}} = 14.70$), CuOH^+ ($pK_{\text{H}} = 7.0$), $\text{Cu}(\text{OH})_2$ ($pK_{\text{H}} = 13.68$), $\text{Cu}(\text{OH})_3^-$ ($pK_{\text{H}} = 17.0$), $\text{Cu}(\text{OH})_4^{2-}$ ($pK_{\text{H}} = 18.50$) were Y^{4-} -ions giving more strong copper trilonat complex – CuY^{2-} ($pK_{\text{H}} = 18.80$) (Lure, 1989). Indium in reaction bath form complexes with following indexes of instability constants InOH^{2+} ($pK_{\text{H}} = 7.55$), $\text{In}(\text{OH})_2^+$ ($pK_{\text{H}} = 17.94$), $\text{In}(\text{OH})_3$ ($pK_{\text{H}} = 26.95$), $\text{In}(\text{OH})_4^-$ ($pK_{\text{H}} = 31.07$), InY^- ($pK_{\text{H}} = 24.95$) (Kumok et al., 1983).

Origin condition of copper (I) sulfide solid phase is essential change with trilon B addition as degree of copper salt transformation to sulfide is decreasing. Thus a velocity of Cu_2S formation decrease, but it almost don't have any change for indium sulfide deposition because trilon B addition in reactor given't a changes in In_2S_3 deposition conditions. It results to formation a more uniform film consisted of particles with average size 50–130 nm.

Growth dynamic of thin film with trilon B addition in mixture (second case of the synthesis) essential differ from first one. Thickness of semiconductor layer $\text{In}_x\text{Cu}_{1-x}\text{S}_y\text{O}_{1-y}$ varying from 115 to 405 nm possesses exponential temperature dependence.

Dark resistance of make-up deposited semiconductor $\text{In}_x\text{Cu}_{1-x}\text{S}_y\text{O}_{1-y}$ in second case of the synthesis is constant in all over temperature interval and equal to 3–5 kOm on a square. One can observe that dark resistance for synthesized films in second case is decreasing from 32 to 8 kOm on a square. Probably this dependence connects with thickness increasing of the semiconductor layers.

Important characteristic of the semiconductor layer promising material in solar cells is a conductivity type. Conductivity type of $\text{In}_x\text{Cu}_{1-x}\text{S}_y\text{O}_{1-y}$ thin films was obtained by means of a thermo-emf sign that in all over intervals of In/Cu ratio and temperature is negative, i.e. a film have p -type conductivity as well as In_2S_3 monocrystal (Bereznev et al., 2013). The individual copper sulfide possess p -type conductivity which full correspond to literature data: Cu_2S is the hole conductor (p -type) (Abrikosov et al., 1975).

Semiconductor p -type material is necessary for creating p - n -junction in solar cells with $\text{In}_x\text{Cu}_{1-x}\text{S}_y\text{O}_{1-y}$ thin films. As p -type semiconductor represent itself a thin films such as lead and tin sulfides deposited by CBD. Also change of semiconductor type is possible by means of a copper quantity varying which is added into $\text{In}_x\text{Cu}_{1-x}\text{S}_y\text{O}_{1-y}$ thin film. Just copper will supply n -type due to excess of that. If CuInS_2 will possess p -type conductivity CdS or GaP thin films can be use for p - n -junction.

4. Conclusion

For the first time $\text{In}_x\text{Cu}_{1-x}\text{S}_y\text{O}_{1-y}$ thin films were deposited by means of CBD in $\text{InCl}_3 - \text{CuCl}_2 - \text{NaOH} - \text{N}_2\text{H}_4\text{CS}$ and $\text{InCl}_3 - \text{CuCl}_2 - \text{Na}_2\text{C}_{10}\text{H}_{14}\text{O}_8\text{N}_2 \cdot 2\text{H}_2\text{O} - \text{NaOH} - \text{N}_2\text{H}_4\text{CS}$ systems at 333–353 K with thickness 115–570 nm and good adhesion to siall substrate. XPS data showed that surface of thin film in $\text{Cu}_2\text{S}-\text{In}_2\text{S}_3$ system include 4.05–9.63 at% of indium, 25.76–49.43 at% of copper, 12.99–26.28 at% of sulfur. Moreover, film composition is including metal oxide phases with 20.12–52.36 at% of oxygen which predicted from ion balance calculation. SEM showed that composition of reaction mixture and deposition temperature depends on morphology of $\text{In}_x\text{Cu}_{1-x}\text{S}_y\text{O}_{1-y}$ nanostructured films. The *n*-type conduction of $\text{In}_x\text{Cu}_{1-x}\text{S}_y\text{O}_{1-y}$ thin films was obtained. The dark resistance varies from 3 to 5 kOm on square meter for deposited films from trilonate-system and from 32 to 8 kOm on square meter for deposited films from second system.

5. Acknowledgements

The research was supported by the Russian Fund of Basis Research (N^o 14-03-00121) and the Ministry of Education and Science of the Russian Federation in the framework of the governmental task N^o 4.1270.2014/K.

References

- Jing-Jing et al., 2012 – Jing-Jing H., Wen-Hui Z., Jie G., Mei L., Si-Xin W. (2012). Inorganic ligand mediated synthesis of CuInS_2 nanocrystals with tunable properties. *Cryst. Eng. Comm.* Vol. 14. pp. 3638-3644.
- Novoselova, 1979 – Novoselova A.V. (1979). Fiziko-himicheskie svoystva poluprovodnikovih vechestv (Physical and chemical properties of semiconductor substances). Moscow: Nauka. 339 p.
- Fiechter, 2008 – Fiechter S. (2008). On the homogeneity region, growth modes and optoelectronic properties of chalcopyrite-type CuInS_2 . *Phys. stat. sol. (b)*. Vol. 245. No. 9. pp. 1761-1771.
- Maier et al., 2011 – Maier E., Rath T., Haas W., Resel R., Trimmel G. (2011). CuInS_2 -Poly(3-(ethyl-4-butanoate)thiophene) nanocomposite solar cells: Preparation by an in situ formation route, performance and stability issues. *Solar Energy Materials and Solar Cells*. Vol. 95. pp. 1354-1361.
- Yanfeng et al., 2011 – Yanfeng C., Shaohua Z., Jinchun J., Shengzhao Y., Junhao C. (2011). Synthesis and characterization of co-electroplated $\text{Cu}_2\text{ZnSnS}_4$ thin films as potential photovoltaic material. *Solar Energy Materials and Solar Cell*. Vol. 95. pp. 2136-2140.
- Kuan-ting et al., 2013 – Kuan-ting C., Chung-Jie C., Dahtong R. (2013). Hydrothermal synthesis of chalcopyrite using an environmental friendly chelating agent. *Materials Letters*. Vol. 98. pp. 270-272.
- Sharma et al., 2009 – Sharma R., Shim S., Mane R., Ganesh T., Ghule A.V., Cai G., Duk-Ho Ham, Sun-Ki Min, Lee W., Sung-Hwan Han (2009). Optimization of growth of ternary CuInS_2 thin films by ionic reactions in alkaline chemical bath as *n*-type photoabsorber layer. *Materials Chemistry and Physic*. Vol. 116. pp. 28-33.
- Lee, JunHo, 2010 – Dong-Yeup Lee, Kim JunHo (2010). Characterization of sprayed CuInS_2 films by XRD and Raman spectroscopy measurements. *Thin solid films*. Vol. 518. pp. 6537-6541.
- Chepra, Das, 1986 – Chepra K.L., Das S.R. (1986). Tonkopenochnii solnechnii elementi (Solar elements from thin films). Moscow: Mir. 435 p.
- Merdes et al., 2011 – Merdes S., Mainz R., Rodriguez-Alvarez H., Klaer J., Klenk R., Meeder A., Schock H.W., Lux-Steiner M.C. (2011). Influence of precursor stacking on the absorber growth in $\text{Cu}(\text{In,Ga})\text{S}_2$ based solar cells prepared by a rapid thermal process. *Thin Solid Films*. Vol. 519. pp. 7189-7192.
- Yoon et al., 2012 – Yoon S.J., Lim I., Kang S.H., Lee W., Han S.-H. (2012). Structural and optical properties of chemically deposited CuInSe_2 thin film in acidic medium. *J. of Nanoscience and Nanotechnology*. V. 12. N^o 5. pp. 4313-4316.
- Fedorova et al., 2015 – Fedorova E.A., Maskaeva L.N., Markov V.F., Ermakov A.N., Samigulina R.F. (2015). Hydrochemical synthesis and thermal stability of nanocrystalline films and precipitates of copper(I) selenide. *Russian Journal of Inorganic Chemistry*. Vol. 60. No. 11. pp. 1311-1316.

[Maskaeva et al., 2012](#) – Maskaeva L.N., Markov V.F., Kuznetsov M.V., Barbin N.M. (2012). Composition and submicron structure of chemically deposited Cu₂Se–In₂Se₃ films. *Technical Physics Letters*. Vol. 38. № 3. pp.290-293.

[Lure, 1989](#) – Lure J.J. The handbook in analytical chemistry. Moscow: Himiy, 1989. 448 p.

[Kumok et al., 1983](#) – Kumok V.N., Kuleshov O.M., Karabin L.A. (1983). Proizvedenay rastvorimosty (Creations of solubility). Novosibirsk: Nauka. 266 p.

[Bereznev et al., 2013](#) – Bereznev S., Adhikari N., Kois J., Kouhiisfahani E., Öpik A. (2013). One-source PVD of n-CuIn₅Se₈ photoabsorber films for hybrid solar cells. *Solar Energy*. Vol. 94. pp. 202-208.

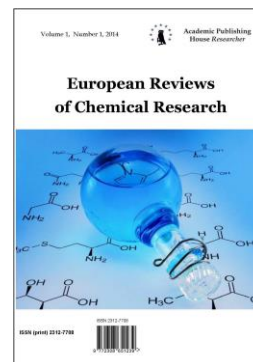
[Abrikosov et al., 1975](#) – Abrikosov N.H., Bankina V.F., Poreckya L.V., Skudnova E.V., Chigevskya S.N. (1975). Poluprovodnicovii hal'kogenidi i splavi na ih osnove (Semiconductors halcogenids and alloys based on them). Moscow: Nauka, 1975. 220 p.

Copyright © 2017 by Academic Publishing House Researcher s.r.o.



Published in the Slovak Republic
European Reviews of Chemical Research
Has been issued since 2014.
ISSN: 2312-7708
E-ISSN: 2413-7243
2017, 4(1): 21-27

DOI: 10.13187/erchr.2017.1.21
www.ejournal14.com



Theoretical Study of the Reactivity and Regioselectivity of the Addition Reaction between HCl and Alkenes, Investigation of the Markovnikov's Rule

Abdellah Zeroual ^{a,*}, Mohamed M. El idrissi ^a, Mohamed Zoubir ^a, Ahmed Benharref ^b

^a Laboratory of Physical Chemistry, Department of Chemistry, Faculty of Science El Jadida, Chouaib Doukkali University, P.O. Box 20, 24000 El Jadida, Morocco

^b Laboratory of Biomolecular Chemistry, Natural Substances and Reactivity, URAC16, Faculty of Sciences Semlalia, Cadi Ayyad University, P.O. Box 2390, Marrakech, Morocco

Abstract

A theoretical study of the mechanism and selectivity of the addition reactions between HCl and alkenes were performed using DFT B3LYP/6-31G(d). Analysis of the global electrophilicity indices shows that the alkene 1-5 behaves as a nucleophile, while HCl behaves as an electrophile. In the addition reaction of the alkenes 1-5 with HCl, the most favorable electrophile-nucleophile interaction will take place between the most nucleophilic centre of alkenes 1-5, the less substituted carbon and most electrophilic centre of HCl, hydrogen atom, in clear agreement with Markovnikov's rule. The calculation of activation and reaction energies indicates that the formations of the Markovnikov's products are favored both kinetically and thermodynamically.

Keywords: Regioselectivity, MEDT, PES, Parr function, Markovnikov rule, DFT B3LYP/6-31G(d).

1. Introduction

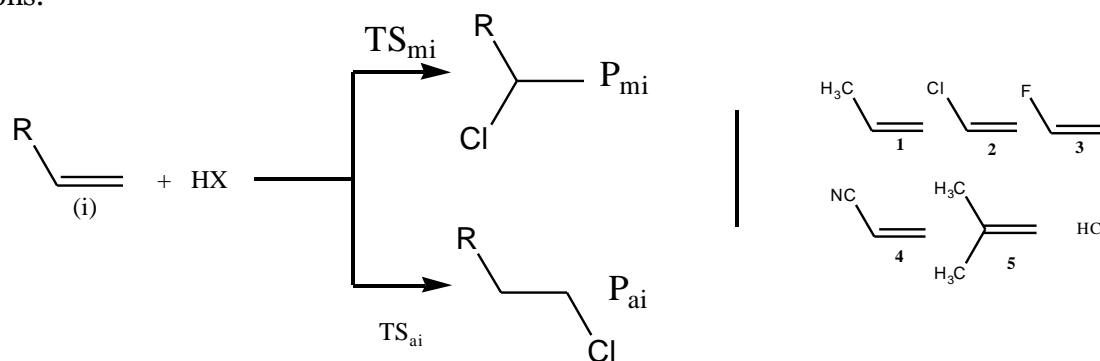
Many halogen compounds are easily synthesized in a highly regio- and stereoselective fashion by an addition reaction between HX and alkenes derivatives (Wang et al., 2015; Stanley et al., 1970; Shengming et al., 1999; Xiaodan et al., 2014; Haiyang et al., 2014; Graham et al., 2009; Marco et al., 2007; BruceM et al.). The hydro-halogenations of an asymmetric alkenes obeys the Markovnikov rule, the proton binds to the least substituted carbon, the reaction is regioselective. In 2008 a distortion/interaction (Ess et al., 2008; Osuna et al., 2009) was introduced by Houk (Houk et al., 2008) to explain the reactivity, this model is analogous of that proposed by Bickelhaupt in 1999 (Bickelhaupt, 1999; Fernández et al., 2014). Houk found that the activation enthalpies correlated very nicely with distortion energies. The partition of the total density of the TS geometry into two separated structure does not have any physical sense within density functional DFT (Hohenberg et al., 1964). Consequently, the energy of two reagents cannot be correlated with the energy of TS because each of them loses the external potential created by the other reagents. The changes in the electron density and not molecular orbital interaction are responsible

* Corresponding author

E-mail addresses: Zeroual19@yahoo.fr (A. Zeroual), idrissi_82@hotmail.fr (M.M. El idrissi), Zjallal@yahoo.fr (M. Zoubir), benharref@ucam.ac.ma (A. Benharref)

for the reactivity in organic molecules (Domingo et al., 2014). Very recently Domingo proposed a new theory to study the reactivity in organic chemistry named Molecular Electron Density Theory (MEDT) (Ríos-Gutiérrez et al., 2015; Domingo et al., 2016).

Herein, in order to understand the effects of the substituent on the molecular mechanism and the reaction rate of the addition reaction between alkenes 1-5 and HCl, as well as the origin of the selectivities experimentally found by Markovnikov's rule (scheme 1), a theoretical characterisation of the molecular mechanism of these zw-type addition reactions is carried out within the MEDT using DFT methods at the B3LYP/6-31G(d) computational level. To this end, besides the exploration and characterisation of the potential energy surfaces (PESs) associated with the studied reactions.



Scheme 1. Addition reaction of the HCl with alkenes.

2. Computational methods

DFT computations were carried out using the B3LYP functional (Zhao et al., 2004), together with the standard 6-31G* basis set. The optimizations have been realized using the Berny analytical gradient optimization method (Schlegel, 1982). All computations have been shown with the Gaussian 09 suite of programs (Frisch et al., 2009). The global electrophilicity index (Parr et al., 1999) ω , was given by the following expression, $\omega = (\mu^2/2\eta)$, in terms of the electronic chemical potential μ and the chemical hardness η . Both quantities could be approached in terms of the one-electron energies of the frontier molecular orbital HOMO and LUMO, ε_H and ε_L , as $\mu = (\varepsilon_H - \varepsilon_L)/2$ and $\eta = (\varepsilon_L - \varepsilon_H)$, respectively (Parr et al., 1983). The empirical (relative) nucleophilicity index N (Jaramillo et al., 2008), based on the HOMO energies obtained within the Kohn–Sham scheme (Kohn et al., 1965), and defined as $N = E_{\text{HOMO}}(\text{Nu}) - E_{\text{HOMO}}(\text{TCE})$. The nucleophilicity was referred to tetracyanoethylene (TCE). This choice allowed us to handle conveniently a nucleophilicity scale of positive values. Electrophilic P^+_k and nucleophilic P^-_k Parr functions (Zeroual et al., 2015; Zeroual et al., 2016; El Idrissi et al., 2016; Zoubir et al., 2017), were obtained through the analysis of the Mulliken atomic spin density (ASD) of the radical anion and radical cation of the reagents. The local electrophilicity indices were evaluated using the following expressions: $N_k = N \cdot P^-_k$. The stationary points were characterised by frequency computations in order to verify that TSs have one and only one imaginary frequency. Intrinsic reaction coordinate (IRC) (Fukui, 1970) pathways were traced to verify the connectivity between minima and associated TSs. Solvent effects of dichloromethane were taken into account through single point energy calculations using the polarisable continuum model (PCM) developed by Tomasi's group in the framework of the self consistent reaction field (Tomasi et al., 1994).

3. Results and discussion

The present theoretical study has been divided in three parts: (1) an analysis of the conceptual DFT indices of the reagents involved in addition reaction of the HCl (hydrochloric acid) with alkenes 1-5. (2) Next, the potential energy surface (PES) associated with the addition reaction of HCl with alkenes 1-5 are explored and characterized, (3) finally a transition states geometries are analyzed.

Analysis of DFT reactivity indices of the reagents involved in the addition reaction of the HCl and alkenes 1-5.

Global DFT indices, namely the electronic chemical potential μ , chemical hardness η , electrophilicity w , and nucleophilicity N are summarized in table 1.

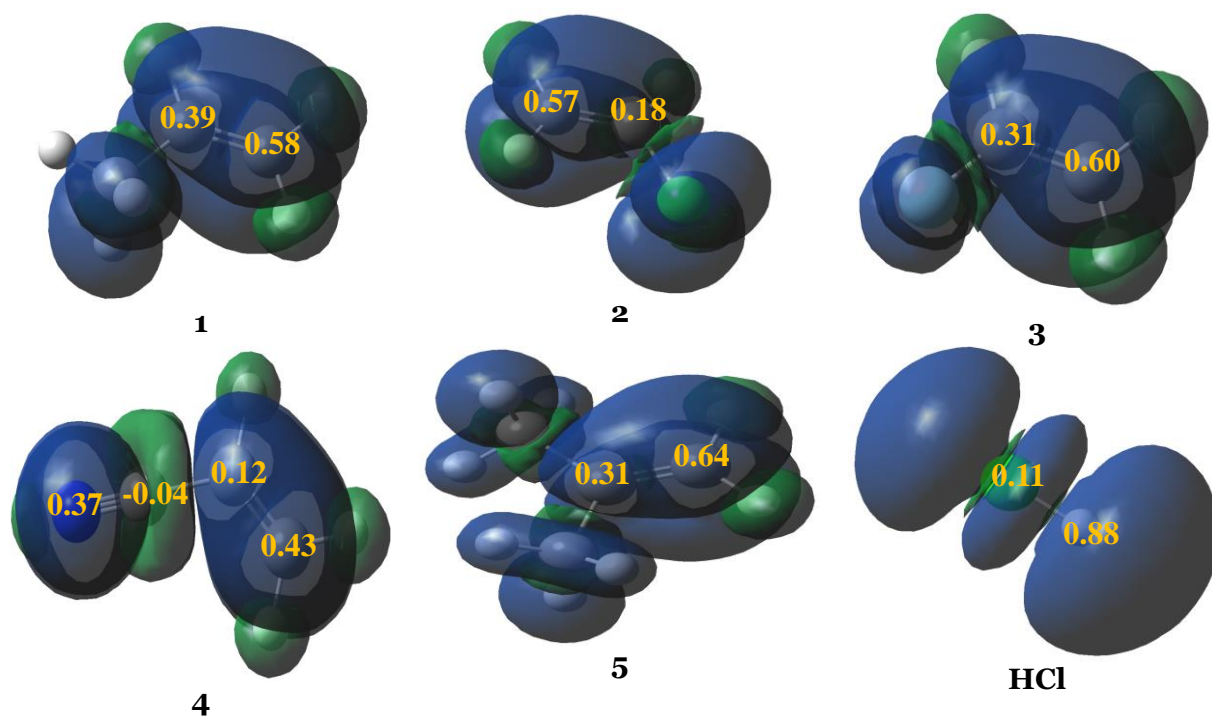
Table 1. Electronic chemical potential, μ , chemical hardness, η , electrophilicity, ω , nucleophilicity, N , indices and pr in eV, of HCl and alkenes 1-5.

Molecule	μ	η	w	N
1	-3.06	7.45	0.63	2.73
2	-3.58	7.10	0.90	2.38
3	-3.26	7.67	0.69	2.43
4	-4.69	6.73	1.63	1.46
5	-2.78	7.41	0.52	3.04
HCl	-4.37	9.28	1.03	0.51

The electronic chemical potential of the alkenes 1-5, -3.06, -3.58, -3.26, -4.09 and -2.78 are higher than that of the HCl, -4.37, indicating that along a polar reaction the global electron density transfer [16] GEDT will flux from the alkenes 1-5 towards the HCl.

The electrophilicity indices of the alkenes 1, 2, 3, and 5 are 0.63, 0.90, 0.69 and 0.52 are smaller than the HCl 1.03 eV, the nucleophilicity indices of the alkenes 1,2,3,4 and 5 are 2.73, 2.38, 2.43, 1.46 and 3.04 are higher than of the HCl 0.51 eV. Consequently, it is expected that HCl participates as a good electrophile and alkenes participates as a good nucleophile.

It has been established that along a polar reaction with non-symmetric reagents the most favourable reactive channel is that where the two-centre interaction is developed between the most electrophilic centre of the electrophile and the most nucleophilic centre of the nucleophile. The electrophilic P_K^+ and the nucleophilic P_K^- Parr functions have been reported as derived from the changes of spin electron density attained by a GEDT process developed from the nucleophile towards the electrophile. According to the Parr functions, the most favourable single bond formation arises between the most electrophilic and nucleophilic centres of the reagents. The electrophilic P_K^+ and nucleophilic P_K^- Parr functions for alkenes 1-5 and HCl are displayed in Fig. 1.

**Fig. 1.** Nucleophilic P_K^- Parr functions of the alkenes 1-5, and electrophilic P_K^+ Parr functions of the HCl

Analysis of the nucleophilic P_K^- Parr functions of the alkenes 1-5 indicates that the carbon not substituted is most nucleophile center of these species and this carbon presenting the maximum

value, $P_K^- = 0.58, 0.57, 0.60, 0.43$ and 0.64 respectively. On the other hand, the electrophilic Parr functions of P_K^+ of HCl indicate that the hydrogen atom is the most electrophilic centre $P_K^+ = 0.88$. Consequently, in the addition reaction of the alkenes 1-5 with HCl, the most favorable electrophile-nucleophile interaction along will take place between the most nucleophile centre of alkenes 1-5, the less substituted carbon and most electrophilic centre of HCl, hydrogen atom, in clear agreement with Markovnikov's rule.

Kinetic study of the addition reaction reaction of alkenes 1-5 and HCl

In order to investigate of the alkenes in the mechanism and regioselectivities of addition reaction between HCl and alkenes 1-5 and examining Markovnikov's rule, the value of enthalpie, the free enthalpie and entropie of the stationry points involved in this addition reaction in gas phase and water are displayed in table 2.

Table 2. The enthalpy (H a.u), the Gibbs free energy (G a.u) and entropy (S cal mol⁻¹ K⁻), computed in gas and water, for the stationary points involved in the addition reaction between the HCl and alkenes 1-5.

	gaz		water	
	G	ΔG	G	ΔG
HCl+ R₁	-578.61054	----	-578.66422	----
TSm ₁	-578.601245	5.83	-578.627343	23.14
TSa ₁	-578.588893	13.58	-578.610363	33.79
Pm ₁	-578.675437	-40.72	-578.680290	-10.08
Pa ₁	-578.672874	-39.11	-578.676532	-7.72
HCl+ R₂	-998.926055	----	-998.981309	----
TSm ₂	-998.907220	11.81	-998.930222	32.05
TSa ₂	-998.895516	19.16	-998.913351	42.64
Pm ₂	-998.987328	-38.44	-998.987326	-10.05
Pa ₂	-998.986126	-37.69	-998.993794	-7.83
HCl+ R₃	-638.554073	----	-638.608905	----
TSm ₃	-638.545601	5.31	-638.569715	24.59
TSa ₃	-638.523234	19.35	-638.542904	41.41
Pm ₃	-638.624902	-44.44	-638.629000	-12.60
Pa ₃	-638.616136	-38.94	-638.620577	-7.32
HCl+ R₄	-631.564522	----	-631.624168	----
TSm ₄	-631.536062	17.85	-631.554284	43.85
TSa ₄	-631.533641	19.37	-631.552620	44.89
Pm ₄	-631.618766	-34.03	-631.625576	-0.88
Pa ₄	-631.616462	-32.59	-631.631941	-4.87
HCl+ R₅	-617.939221	----	-617.949274	----
TSm ₅	-617.902622	22.96	-617.933615	9.82
TSa ₅	-617.879759	37.31	-617.901448	30.01
Pm ₅	-617.965970	-16.78	-617.953840	-2.86
Pa ₅	-617.960549	-13.38	-617.964097	-9.30

The gas-phase activation with the two competitive channels are 5.83 (TSm₁) and 13.58 (TSa₁) kcal/mol, the reaction being exothermic by 40.72 and 39.11 kcal/mol, consequently, it can be considered irreversible. This energy result is formed by kinetic and thermodynamic control.

The activation free energies with the competitive channels of the reaction between HCl and R₂ are 11.81 (TSm₂) and 19.66 (TSa₂) kcal/mol, indicating that the Pm₂ is kinetically favored, this reaction being exothermic by 38 Kcalmol⁻¹, consequently, this reaction can be irreversible.

The activation Gibbs free energy of the stationary points involved in this addition reaction between HCl and R₃ are 5.31 (TSm₃) and 19.35 (TSa₃) kcal/mol, the formation Gibbs free energies of the products are 44.44 (Pm₃) and 38.94 kcal/mol (Pa₃), the formation of the product Pm₃ is

strongly exergonic than Pa3 by 5.50 kcal/mol, consequently the formation of the product Pm3 is kinetically and thermodynamically very favored.

The activation Gibbs free energies of the stationary points involved in reaction HCl and R4 are 17.85 (Tsm4) and 19.37 Kcal/mol(TSa4), this energy result indicate that the formation of the product Pm4 is kinetically favored, in addition the reaction being exothermic by 34.06 (Pm4) and 32.59 kcal/mol (Pa4) is thermodynamically favored too.

The activation Gibbs free energies associated with Tsm5 and TSA5 are 22.96 and 37.31 kcal/mol respectively, the reaction being exothermic by 16.78 (Pm5) and 13.38 kcal/mol (Pa5), this energy result indicate that the formation of the product Pm5 is kinetically and thermodynamically favored in good agreement with Markovnikov's rule.

Inclusion of solvent effects of water increases the gas phase activation energies by 17.31 (Tsm1), 20.21 (Tsa1), 20.24 (Tsm2), 23.48 (Tsa2), 19.28 (Tsm3), 22.06 (Tsa3), 26.00 (Tsm4), 25.52 (Tsa4), 13.14 (Tsm5) and 7.03 (Tsa5) kcal/mol and slightly decreases the exothermic character of the reaction by 30.64 (Pm1), 31.39 (Pa1), 25.84 (Pm2), 29.86 (Pa2), 31.80 (Pm3), 31.62 (Pa3), 33.15 (Pm4), 18.72 (Pa4), 13.92 (Pm5) and 4.08 (Pa5), these effects are consequence of the better salvation of addition reaction between HCl and alkenes in this polar solvent. In this case, while the Markovnikov's regioselectivity is increased

The lengths of the forming bonds in the geometries of the TSs involved in the two competitive reaction channels in water are also included in Fig. 2. A comparison of the lengths of the C–C forming bonds obtained in gas phase and water indicates that there are no significant differences. The most favorable TS-m1, TS-m2, TS-m3, TS-m4, TS-m5 and TS-m6 becomes slightly more asynchronous, since the H–C distance increases by 0.1 Å. Consequently, the inclusion of solvent effects of water modifies neither the relative energies nor the C–Cl single bond formation at the TSs.

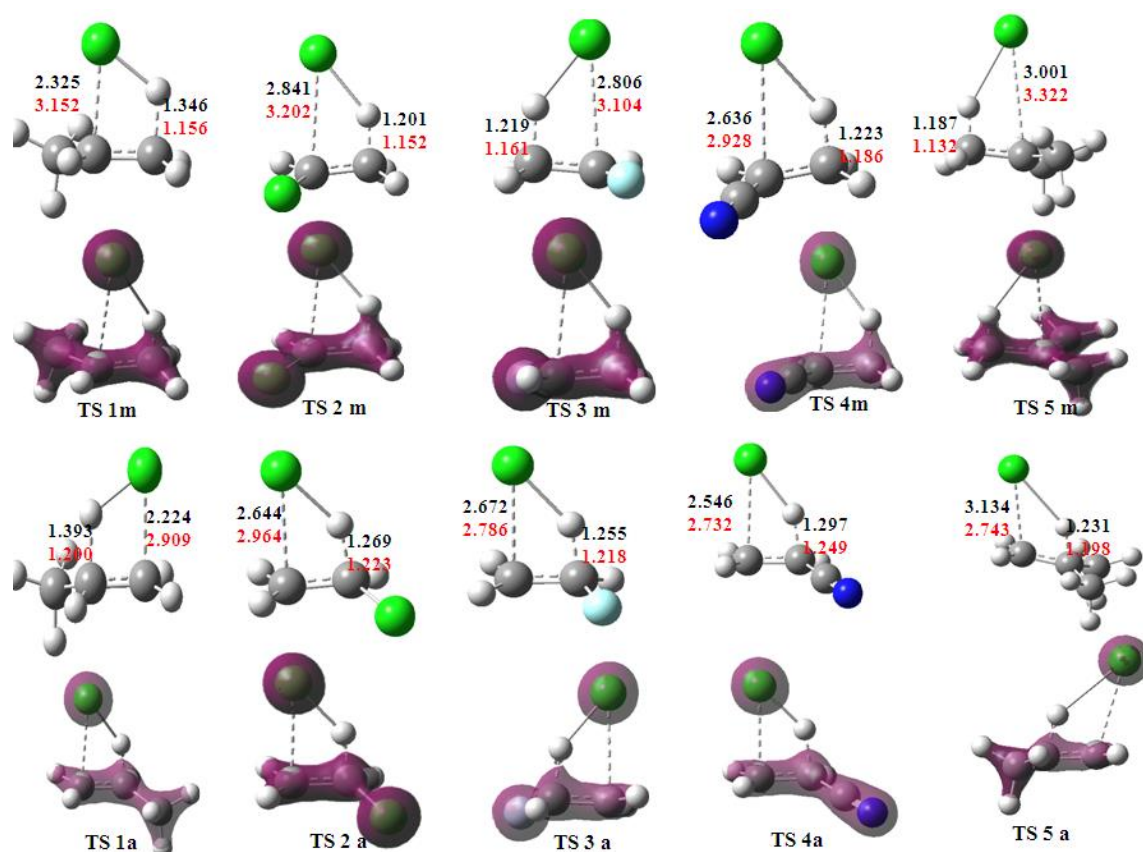


Fig. 2. DFT/6-31G(d) optimized density map and structures of the TSs of the addition reaction between the HCl and alkenes 1-5. Lengths are given in Angstroms.

4. Conclusion

The addition reaction of HCl with ethylene 1-5 has been studied within the MEDT through DFT calculations at the B3LYP/6-31G(d) computational level. The obtained results are supported by the combination of the analysis of the reactivity indices at the ground state of the reagents, derived from the conceptual DFT, the exploration of the energies associated with this addition reaction along the corresponding reactive channels. Analysis of the nucleophilic P_k^- Parr functions allows characterizing the C carbon atom as the most nucleophilic centre of 1-5, in clear agreement with the regioselectivity found in Markovnikov's rule. An exploration of the energies associated with this addition reaction indicates this addition reaction is high regioselectivity and Markovnikov's products are kinetically and thermodynamically favored.

References

- Bruce et al., 2008 – Bruce M. Bell, John R. Briggs, Robert M. Campbell, Susanne M. Chambers, Phil D. Gaarenstroom, Jeffrey G. Hippler, Bruce D. Hook, Kenneth Kearns, John M. Kenney, William J. Kruper, D. James Schreck, Curt N. Theriault, Charles P. Wolfe. (2008). Glycerin as a Renewable Feedstock for Epichlorohydrin Production. *The GTE Proc, Clean*, 36 (8): 657–661.
- Bickelhaupt et al., 1999 – Bickelhaupt F M. (1999). Understanding reactivity with Kohn–Sham molecular orbital theory: E2–SN2 mechanistic spectrum and other concepts. *J Comput Chem*; 20:114–128.
- Domingo et al., 2014 – Domingo L R. (2014). A new C–C bond formation model based on the quantum chemical topology of electron density. *RSC Adv*. 4:32415–32428.
- Domingo et al., 2016 – Domingo L R, Ríos-Gutiérrez M, Pérez P. (2016). A new model for C–C bond formation processes derived from the Molecular Electron Density Theory in the study of the mechanism of [3+2] cycloaddition reactions of carbenoid nitrile ylides with electron-deficient ethylenes. *Tetrahedron*. 72:1524–1532.
- El Idrissi et al., 2016 – M. El Idrissi, M. Zoubir, A. Zeroual, R. El Ajlaoui, A. El Haib, A. Benharref, A. Elhajbi. (2016). A theoretical study of the mechanism and regioselectivity of the 1,3-dipolar cycloaddition reaction of azides with alkynes. *J. MAR.CHIM. HETEROCYCL*. 15(1): 145–151.
- Ess et al., 2008 – Ess D H, Houk K N. (2008). Theory of 1,3-Dipolar Cycloadditions: Distortion/Interaction and Frontier Molecular Orbital Models. *Journal of American Chemical Society*. 130:10187–10198.
- Ess et al., 2015 – Ess D H, Houk K N (2007). Distortion/Interaction Energy Control of 1,3-Dipolar Cycloaddition Reactivity. *Journal of American Chemical Society*. 129 (35), 10646–10647.
- Fernández et al., 2014 – Fernández I, Bickelhaupt F M. (2014). The activation strain model and molecular orbital theory: understanding and designing chemical reactions. *Chemical Society Reviews*. 43:4953–4967.
- Frisch et al., 2009 – Frisch M J et al., Gaussian 09, Revision A 02, Gaussian Inc., Wallingford CT, 2009.
- Fukui et al., 2009 – Fukui K. (1970). Formulation of the reaction coordinate. *J. Phys. Chem*. 74: 4161–4163.
- Graham et al., 2009 – Graham J. Hutchings. (2009). Nanocrystalline gold catalysts: A reflection on catalyst discovery and the nature of active sites, *Gold Bulletin*. 42 (4): 260-266.
- Haiyang et al., 2009 – Haiyang Zhang, Bin Dai, Wei Li, Xugen Wang, Jinli Zhang Mingyuan Zhu, Junjie Gu. (2014). Non-mercury catalytic acetylene hydrochlorination over spherical activated-carbon-supported Au–Co(III)–Cu(II) catalysts. *Journal of Catalysis*. 316:141–148.
- Hammond, 2009 – Hammond G S. (1955). A Correlation of Reaction Rates. *J Am Chem Soc*. 77:334–338.
- Hohenberg et al., 2009 – Hohenberg P, Kohn W. (1964). Inhomogeneous Electron Gas. *Phys Rev B* 136:864–871.
- Jaramillo et al., 2009 – Jaramillo P, Domingo L R, Chamorro E, Pérez P. (2008). further exploration of a nucleophilicity index based on the gas-phase ionization potentials. *J. Mol. Struct*. 865: 68 –72.

Kohn et al., 2009 – Kohn W, Sham L. (1965). Self-Consistent Equations Including Exchange and Correlation Effects, *J. Phys. Rev.* 140: 1133-1138.

Marco et al., 2007 – Marco Conte, Albert F. Carley, Clare Heirene, David J. Willock, Peter Johnston, Andrew A. Herzing, Christopher J. Kiely, Graham J. Hutchings. (2007). Hydrochlorination of acetylene using a supported gold catalyst: A study of the reaction mechanism. *Journal of Catalysis.* 250: 231–239.

Osuna et al., 2009 – Osuna S, Houk K N. (2009). Cycloaddition Reactions of Butadiene and 1,3-Dipoles to Curved Arenes, Fullerenes, and Nanotubes: Theoretical Evaluation of the Role of Distortion Energies on Activation Barriers. *Chem Eur J* 15:13219–13231.

Parr et al., 1999 – Parr R.G, Szentpaly L V, Liu S. (1999). Electrophilicity Index, *J. Am. Chem. Soc.* 121: 1922-1924.

Parr et al., 1983 – Parr R G, Pearson R G. (1983). Absolute Hardness: Companion Parameter to Absolute Electronegativity, *J. Am. Chem. Soc.* 105 7512 -7516.

Ríos-Gutiérrez et al., 2015 – Ríos-Gutiérrez M, Domingo L R, Pérez P. (2015). Understanding the high reactivity of carbonyl compounds towards nucleophilic carbenoid intermediates generated from carbene isocyanides. *RSC Adv*, 5: 84797–84809.

Shengming et al., 1999 – Shengming Ma ,Lintao Li , and Hexin Xie. (1999). Hydrohalogenation Reaction of 1,2-Allenyl Ketones Revisited. Efficient and Highly Stereoselective Synthesis of β,γ -Unsaturated β -Haloketones, *J. Org. Chem.* 64 (14): 5325–5328.

Stanley et al., 1970 – Stanley R. Sandler. (1970). Cyanuric chloride. Novel laboratory hydrochlorinating reagent for alcohols, *J. Org. Chem.* 35 (11): 3967–3968.

Schlegel, 1982 – Schlegel H B. (1982). Optimization of Equilibrium Geometries and Transition Structures, *J. Comput. Chem.* 2 214 218.

Tomasi et al., 1994 – Tomasi J, Persico M. (1994). Molecular Interactions in Solution: An Overview of Methods Based on Continuous Distributions of the Solvent, *Chem. Rev.* 94: 2027–2094.

Wang et al., 2015 – Wang Lu, Feng Wang, Jide Wang. (2015). Catalytic properties of Pd/HY catalysts modified with NH₄F for acetylene hydrochlorination, *Catalysis Communications*, 65(5): Pages 41–45.

Xiaodan et al., 2014 – Xiaodan Yang, Chunhai Jiang, Zhenming Yang, Jinsong Zhang. (2014). Hydrochlorination of Acetylene Using SiC Foam Supported Structured C/Au Catalysts, *Journal of Materials Science & Technology*, 30(5): 434–440.

Zeroual et al., 2015 – Zeroual A, Benharref A, El Hajbi A. (2015). Theoretical study of stereoselectivity of the [1+2] cycloaddition reaction between (1S,3R,8S)-2,2-dichloro-3,7,7,10-tetramethyltricyclo[6,4,0,0^{1,3}]dodec-9-ene and dibromocarbene using density functional theory (DFT) B3LYP/6-31G*(d), *J Mol Model*, 21: 2594-2599.

Zeroual et al., 2015 – Zeroual A, El Haib A, Benharref A, El Hajbi A. (2015), A combined experimental and theoretical study of highly chemoselectivity acetylation of diterpene, *JCMMDA*. 5: 58-62.

Zeroual et al., 2015 – Zeroual A, Zoubir M, Hammal R, Benharref A, El Hajbi A. (2015). Understanding the regioselectivity and reactivity of Friedel–Crafts benzoylation using Parr functions, *Mor. J. Chem.* 3: 356-360.

Zhao et al., 2004 – Zhao Y, Truhlar D G. (2004). Hybrid Meta Density Functional Theory Methods for Thermochemistry, Thermochemical Kinetics and Noncovalent Interactions: The MPW1B95 and MPWB1K Models and Comparative Assessments for Hydrogen Bonding and van der Waals Interactions, *J. Phys. Chem. A*, 108: 6908 -6918.

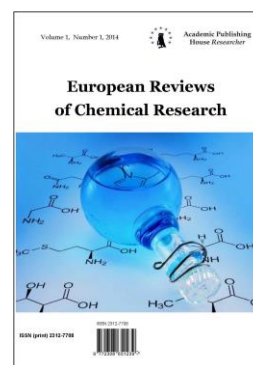
Zoubir et al., 2014 – Zoubir M, Zeroual A, El Idrissi M, El Haib A, Moumou M, Hammal R, Mazoir N, Benharref A, El Hajbi A. (2017). Understanding the Chemoselectivity and Stereoselectivity in Michael Addition Reactions of β -Hydroxyparthenolides and Amines such as Pyrrolidine, Morpholine, Piperidine and 1-Methylpiperazine: a DFT Study, *Journal of Materials and Environmental Sciences*, 8: 990-996.

Copyright © 2017 by Academic Publishing House Researcher s.r.o.



Published in the Slovak Republic
European Reviews of Chemical Research
Has been issued since 2014.
ISSN: 2312-7708
E-ISSN: 2413-7243
2017, 4(1): 28-33

DOI: 10.13187/erchr.2017.1.28
www.ejournal14.com



Theoretical Investigation of the Chemo and the Regioselectivity of the Reaction Oxidation of Bicyclo[3.2.0]Hept-2-En-6-One by Hydrogen Peroxide

M. Zoubir ^a, M. El Idrissi ^a, R. El Ajlaoui ^c, A. El Haib ^b, S. Abouricha ^d, A. Zeroual ^{a, b*1,2*}, A. Benharref ^b, A. El Hajbi ^a

^a Laboratory of Physical Chemistry, Department of Chemistry, Faculty of Science Chouaib Doukkali University, EL Jadida, Morocco

^b Laboratory of Biomolecular Chemistry, Natural Substances and Reactivity, URAC 16 Semlalia Faculty of Sciences, Cadi Ayyad University, Marrakech, Morocco

^c Laboratory of Organic and Analytical Chemistry, Faculty of Sciences and Techniques, Sultan Moulay Slimane University, P.O. Box 523, Beni-Mellal, Morocco

^d Laboratory of Interdisciplinary Research in Science and Technology, P.O. Box 592, 2300, Poly Disciplinary Faculty, Sultan Moulay Slimane, University, Beni Mellal Morocco

Abstract

The mechanism, the chemoselectivity and regioselectivities of the oxidation reaction of bicyclo[3.2.0]hept-2-en-6-one and hydrogen peroxide, have been studied using B₃LYP DFT methods together with the standard 6-31(d) basis set. The potential energy surface (PES) was analyzed by considering the chemo and regio-isomeric Pathways, we found that this reaction was chemo and regioselective and regioisomer P₁ is kinetically and thermodynamically favored in good agreement with experimental Result, in addition the analysis of the potential electrostatic and Parr functions confirming this result.

Keywords: regioselective, PES, chemoselective, the potential electrostatic.

1. Introduction

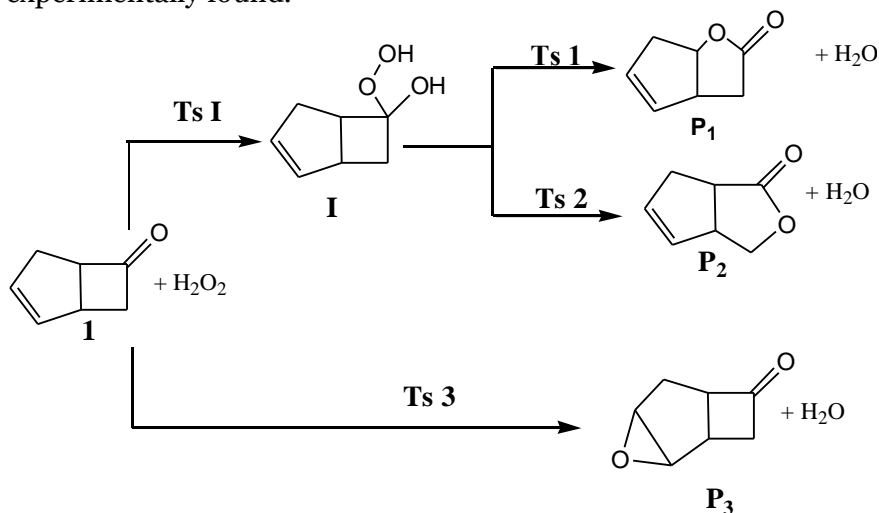
The Baeyer-Villiger (B.V) oxidation is one the most important reaction in therapeutic and organic chemistry based on oxidation of ketones to esters by peracids like as m-CPBA (Zaki et al., 2015), this reaction has high synthetic value and has been used in various synthesis and hemi-synthesis. In particular is a useful for synthesis optically and active lactones because this reaction was highly stereo and regioselective (Marco et al., 2014). In recent years, an attempt was made to change the traditional peroxyacids with green and environmentally friendly peroxide like hydrogen peroxide H₂O₂ or O₂ (House et al., 1972; Krow, 1993; Ten Brink et al., 2004; Zhou et al., 2014; Renz, Meunier, 1999).

C. Mazzini et al. experimentally studied the B-V reaction between bicyclo[3.2.0]hept-2-en-6-one and hydrogen peroxide (Mazzini et al., 1996), finding that this reaction is chemio and regioselective yielding the corresponding lactone P₁ (3,3a,6,6a-tetrahydro-cyclopenta[b]furan-2-one) as the major chemio and regioisomere (see Scheme 1).

* Corresponding author

E-mail addresses: zeroual19@yahoo.fr (A. Zeroual)

Herein, a DFT study of B-V reaction between bicyclo[3.2.0]hept-2-en-6-one and hydrogen peroxide yielding 3,3a,6,6a-tetrahydro-cyclopenta[b]furan-2-one, experimentally studied by C. Mazzini et al. our aim is to perform a theoretical study of the reaction mechanism of this reaction yielding the final product P₁, as well as to explain the chemo- and regioselectivity experimentally found.



Scheme 1. Competitive chemo and regio-isomeric pathways associated with the reaction of bicyclo[3.2.0]hept-2-en-6-one by hydrogen peroxide.

2. Materials and methods

All the calculations were carried out using Gaussian 09 program. Exploration of the potential energy surface (PES) associated with B-V reaction between bicyclo[3.2.0]hept-2-en-6-one and hydrogen peroxide was carried out using the B3LYP functional (Zhao et al., 2004) together with the 6-31(d) basis set (Hehre et al., 1986). The optimizations were carried out using Berny analytical gradient optimization method (Schlegel, 1982). The stationary points were characterized by frequency calculations to verify that the transition states (TSS) had one imaginary frequency. The IRC paths (Fukui, 1970) were traced to verify the energy profiles connecting to the two associated minima.

The global electrophilicity index (Parr et al., 1999) ω , was given by the following expression, $\omega = (\mu^2/2\eta)$, in terms of the electronic chemical potential μ and the chemical hardness η , such as $\mu = (\epsilon_H - \epsilon_L)/2$ and $\eta = (\epsilon_L - \epsilon_H)$ (Parr et al., 1983). The empirical nucleophilicity index N (Jaramillo et al., 2008), based on the HOMO energies obtained within the Kohn-Sham, and defined as $N = E_{HOMO}(Nu) - E_{HOMO}(TCE)$. Electrophilic P_k^+ and nucleophilic P_k^- Parr functions (Zeroual et al., 2015; 2015; Domingo et al., 2015; Zoubir et al., 2017; Ourhriss et al., 2017), were obtained from the analysis of the Mulliken atomic spin density (ASD) of the radical anion and radical cation of the reagents. The local electrophilicity and local nucleophilicity indices were evaluated using the following expressions: $w_k = wP_k^+$, $N_k = NP_k^-$.

The electrostatic potential is a real property, a physical observable. It can be obtained computationally (Stewart, 1979). While it has been used to interpreting and predicting the regioselectivity (Murray et al., 2011). Regions where $V(r) > 0$ can be expected to be attracted favorably, at least initially, to negative portions of other molecules, while $V(r) < 0$ predicts attractive interactions with positive portions.

3. Results and discussion

The present study has been divided into two sections: i) first, the Baeyer-Villiger reaction between bicyclo[3.2.0]hept-2-en-6-one and hydrogen peroxide is theoretically investigated. The energetic aspects, geometrical parameters of the TSS, ii) Parr functions maps and their electrostatic potential maps are analyzed.

3.1. Kinetic study of the oxidation reaction of bicyclo[3.2.0]hept-2-en-6-one by hydrogen peroxide.

The values of the Gibbs free energies and the relative of the stationary points involved in the B-V reaction between bicyclo[3.2.0]hept-2-en-6-one and hydrogen peroxide are summarized in Table 1. The Gibbs free energy profile of the B-V reaction between bicyclo[3.2.0]hept-2-en-6-one and hydrogen peroxide is given in Figure 1.

Table 1. DFT/6-31G(d) Gibbs free energies (G, in a.u.), and the relative a (ΔG in kcal mol⁻¹), for the stationary points involved in the B-V reaction between bicyclo[3.2.0]hept-2-en-6-one and hydrogen peroxide.

System	G	ΔG
1 + H₂O₂	-498.159264	-----
TS I	-498.059572	62.55
TS 3	-498.0532548	66.52
I	-498.150476	5.51
P 3 + H₂O	-498.229288	-43.94
TS 1	-498.069572	56.28
TS 2	-498.058301	63.35
P 1 + H₂O	-498.293184	-84.03
P 2 + H₂O	-498.289508	-81.72

• **Competition between epoxydation and B V (chemo-selectivite)**

The activation energies associated with epoxydation and B V are 66.52 (TS 3), and 62.55 (TS I) kcal mol⁻¹, these energy results indicate that the formation of intermediate I is kinetically favored. Consequently, due to the strong chemoselectivity character of this reaction and the formation of the product P1 is thermodynamically favored than product P3.

• **Understanding the regioselectivity of the B V reaction between bicyclo[3.2.0]hept-2-en-6-one and hydrogen peroxide.**

The activation Gibbs free energy corresponding to the formation the products P1 and P2 are 56.28 (TS 1), and 63.35(TS 2) kcal mol⁻¹ favouring kinetically the formation of P1 as the single lactones, in good agreement with the experimental observations. Note that while formation of the products P1 and P2 are exothermic by 84.03 and 81.72 kcal mol⁻¹ respectively; consequently, the product P1 is kinetically and thermodynamically favored.

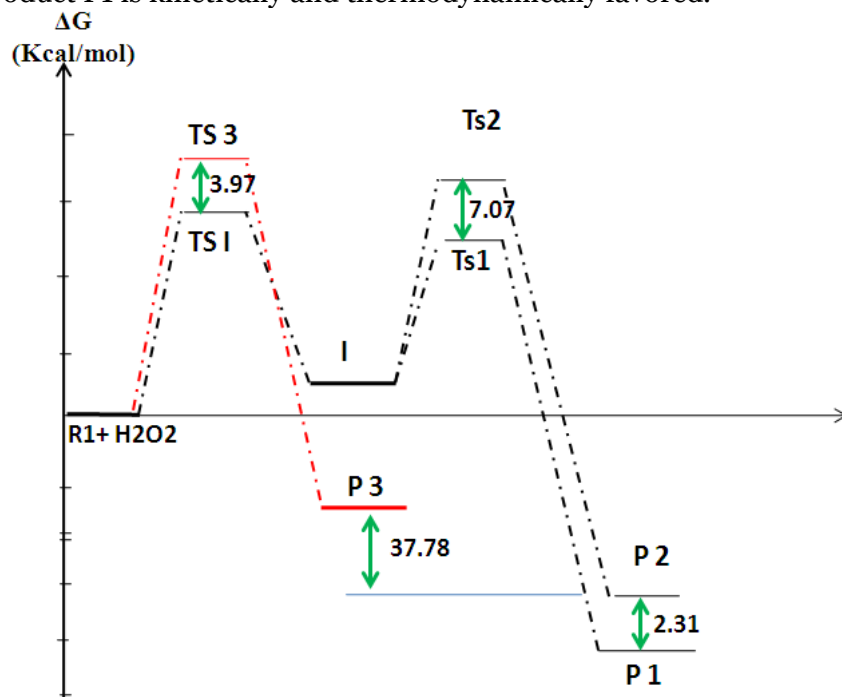


Fig. 1. Gibbs free energy profile (ΔG , in kcal mol⁻¹) of the reaction between the ketone 1 and hydrogen peroxide.

The geometries of the TSs involved in the reaction between bicyclo[3.2.0]hept-2-en-6-one and hydrogen peroxide are given in Figure 2. The lengths of the O-H forming bonds at the TSs TS-3 and TS-I, are 1.676 Å and 1.419 Å respectively, the lengths of the O-C forming bonds at the TSs TS-1 and TS-2, are 2.111 Å and 2.135 Å respectively. These geometric parameters suggest an asynchronous bond formation process along the most favorable P1 regioisomeric channel.

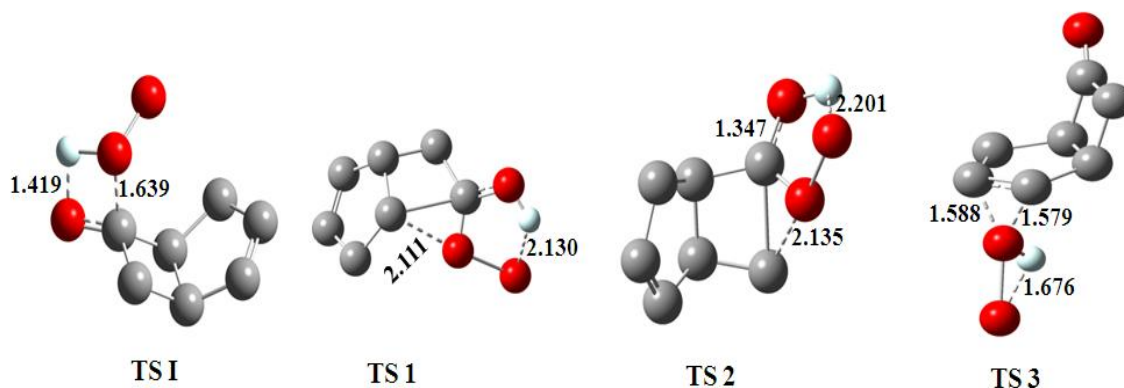


Fig. 2. DFT/6-31G(d) optimized structures of the TSs of the bicyclo[3.2.0]hept-2-en-6-one and hydrogen peroxide. Lengths are given in Angstroms.

3.2. Understanding the chemoselectivity of this reaction using electrostatic potential $V(r)$ and Parr functions.

The global DFT indices, namely the electronic chemical potential μ , chemical hardness η , electrophilicity ω and nucleophilicity N , are given in table 2.

Table 2. B3LYP/6-31G(d) electronic chemical potential, chemical hardness, electrophilicity and nucleophilicity in eV, of the ketone R-1 and hydrogenperoxid

	μ	η	N	ω
H ₂ O ₂	-3.06	7.27	2.82	0.64
R-1	-3.54	5.96	3.00	1.05

We can observe from Table 1 that the electronic chemical potential of hydrogen peroxide H₂O₂ -3.06 is higher than that of ketone R-1 -3.054 eV, indicating that the global electron density transfer (GEDT) will flux from H₂O₂ framework towards ketone R-1.

We are looked from Table 1 that the electrophilicity and nucleophilicity of the ketone R-1 are higher than electrophilicity and nucleophilicity of H₂O₂ the fact that the most favourable reactive channel is that involving the initial two-centers interaction between the most electrophilic centre and most nucleophilic centre of the reagents.

The nucleophilic P_k^- Parr function, the electrophilic P_k^+ Parr function and the electrostatic potential of the reagents were analyzed in order to characterize the most electrophilic and nucleophilic centers of the species involved in this reaction, and, thus, to explain the chemoselectivity experimentally observed (Fig. 3).

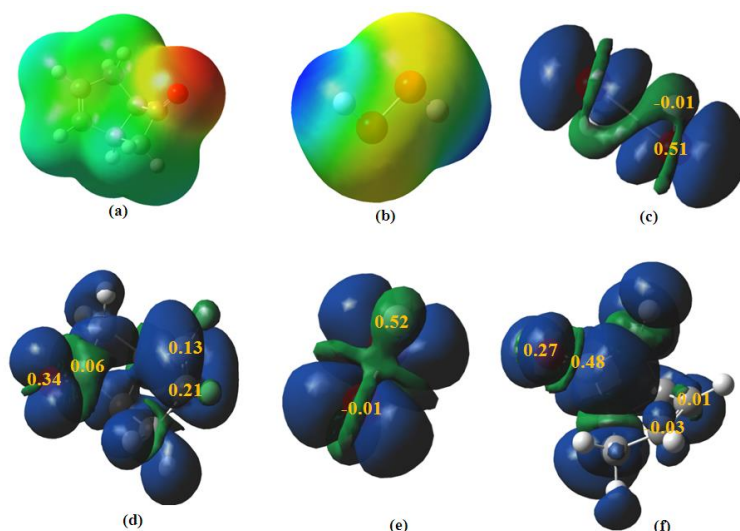


Fig. 3. (a) and (b) electrostatic potential, (c) and (f) the electrophilic Parr function maps, (d) and (e) the nucleophilic Parr function maps of the reagents R1 and H₂O₂, respectively

Analysis of the electrostatic potential maps of reagents indicating that the oxygen atom of the ketone is the most nucleophilic center of this ketone presenting red color and the hydrogen atom of hydrogenperoxid is the most electrophilic center presenting blue color. So the best interaction take place between oxygen atom of the ketone and hydrogen atom of peroxide H₂O₂. On the other hand the The nucleophilic P_k^- Parr function, the electrophilic P_k^+ Parr function of the ketone R-1 indicate that the oxygen atom is the most nucleophilic center $P_k^- = 0.34$ and C7 atom is most electrophilic center $P_k^+ = 0.48$ and for the hydrogen peroxide the nucleophilic P_k^- Parr function, the electrophilic P_k^+ Parr function indicate that the oxygen of this specie is the most nucleophilic center $P_k^- = 0.51$ and hydrogen atom is the electrophilic center $P_k^+ = 0.56$.

Consequently, in this oxidation reaction of the ketone R-1 by hydrogenperoxide H₂O₂, the most favourable electrophile-nucleophile interaction will take place between oxygen of the ketone with hydrogen of hydrogen peroxide and between C7 atom of the ketone and oxygen of peroxide. In clear agreement with the total chemoselectivity experimentally observed.

4. Conclusion

The high chemo and regioselectivity of ketone R-1 towards the lactones P₁ by the B V reaction, has been studied using DFT methods at the B3LYP/6-31(d). Analysis of the relative Gibbs free energies, Parr functions and the electrostatic potential indicates that while the formation of the products P₁ is favorable.

References

- [Domingo et al., 2015](#) – Domingo L. R. Aurell M. J. Pérez P. (2015). A mechanistic study of the participation of azomethine ylides and carbonyl ylides in [3+ 2] cycloaddition reactions; *Tetrahedron*, 71: 1050-1057.
- [Fukui, 1970](#) – Fukui K. (1970). Formulation of the reaction coordinates. *J. Phys. Chem.*, 74: 4161-4163.
- [Hehre et al., 1986](#) – Hehre W.J. Radom L. Schleyer P.V.R. Pople J.A. (1986). Ab Initio Molecular Orbital Theory, Wiley, New York.
- [House et al., 1972](#) – House H. O. (1972). Modern Synthetic Reactions, 2nd ed.; Benjamin: Menlo Park, CA,; 306-307 and 321-328.
- [Jaramillo et al., 2008](#) – Jaramillo P. Domingo L.R. Chamorro E. Pérez P. (2008). A further exploration of a nucleophilicity index based on the gas-phase ionization potentials. *J. Mol. Struct.* 865: 68 –72.
- [Kohn et al., 1965](#) – Kohn W., Sham L. (1965). Self-consistent equations including exchange and correlation effects. *J. Phys. Rev.* 140: 1133-1138.

- [Krow, 1993](#) – Krow G. R. (1993). The Baeyer–Villiger oxidation of ketones and aldehydes. *Org. React.*, 43: 251-798.
- [Marco et al., 2014](#) – De S. R. Kumar G. Jat J. L. Birudaraju S. Lu B. Manne R. Puli N. Adebessin A. M. Falck J.R. (2014). Regio- and stereoselective monoepoxidation of dienes using methyltrioxorhenium: Synthesis of allylic epoxides. *J. Org. Chem.* 79: 10323–10333.
- [Mazzini et al., 1996](#) – Mazzini C. Iebretton J. Furstoss R. (1996). Flavin-Catalyzed Baeyer–Villiger Reaction of Ketones: Oxidation of Cyclobutanones to γ Lactones Using Hydrogen Peroxide. *J. Org. Chem.* 61 8-9.
- [Murray et al., 2011](#) – Murray J.S. Politzer P. (2011). The electrostatic potential: an overview. *WIREs Comp. Mol. Sci.* 1: 153–163.
- [Ourhriss et al., 2017](#) – Ourhriss N., Zeroual A. (2017). Ait Elhad M. Mazoir N. Abourriche A. Gadhi C. A. Benharref A. El Hajbi A. Synthesis of 1-isopropyl-4,7-dimethyl-3-nitronaphthalene: An experimental and theoretical study of regiospecific nitration. *Journal of Materials and Environmental Sciences.* 8 (4) 1385-1390.
- [Parr et al., 1983](#) – Parr R.G. Pearson R.G. (1983). Absolute hardness: companion parameter to absolute electronegativity. *J. Am. Chem. Soc.* 105: 7512-7516.
- [Parr et al., 1999](#) – Parr R.G. Szentpaly L. V. Liu S. (1999). Electrophilicity index. *J. Am. Chem. Soc.* 121: 1922-1924.
- [Renz et al., 1999](#) – Renz M., Meunier B. (1999). 100 years of Baeyer-Villiger oxidations. *Eur. J. Org. Chem.* 737-750.
- [Schlegel, 1982](#) – Schlegel H.B. (1982). Optimization of equilibrium geometries and transition structures. *J. Comput. Chem.*, 2: 214–218.
- [Stewart, 1979](#) – Stewart R.F. (1979). On the mapping of electrostatic properties from Bragg diffraction data. *Chem. Phys. Lett.* 65 (1979) 335–342.
- [Ten Brink et al., 2004](#) – Ten Brink G.-J. Arends I. W. C. E. Sheldon R. A. (2004). The Baeyer–Villiger reaction: New developments toward greener procedures. *Chem. Rev.*, 104: 4105-4123.
- [Zaki et al., 2015](#) – Zaki M. Tebbaa M. Hiebel M. A. Benharref A. Akssira M. Berteina-Raboin S. (2015). Acid-promoted opening of 4,5- and 3,4-epoxy eudesmane scaffolds from α -isocostic acid. *Tetrahedron*, 71: 2035–2042.
- [Zeroual et al., 2015](#) – Zeroual A, Benharref A, El Hajbi A. (2015). Theoretical study of stereoselectivity of the [1+2] cycloaddition reaction between (1S,3R,8S)-2,2-dichloro-3,7,7,10-tetramethyltricyclo[6,4,0,0¹⁻³]dodec-9-ene and dibromocarbene using density functional theory (DFT) B3LYP/6-31G*(d), *J Mol Model*, 21: 2594-2599.
- [Zeroual et al., 2015](#) – Zeroual A, El Haib A, Benharref A, El Hajbi A. (2015), A combined experimental and theoretical study of highly chemoselectivity acetylation of diterpene, *JCMMDA*. 5: 58-62.
- [Zeroual et al., 2015](#) – Zeroual A, Zoubir M, Hammal R, Benharref A, El Hajbi A. (2015). Understanding the regioselectivity and reactivity of Friedel–Crafts benzoylation using Parr functions, *Mor. J. Chem.* 3: 356-360.
- [Zhao et al., 2004](#) – Zhao Y. Truhlar D.G. (2004). Hybrid Meta Density Functional Theory Methods for Thermochemistry, Thermochemical Kinetics, and Noncovalent Interactions: The MPW1B95 and MPWB1K Models and Comparative Assessments for Hydrogen Bonding and van der Waals Interactions. *J. Phys. Chem., A* 108: 6908–6918.
- [Zhou et al., 2014](#) – Zhou L. Liu X. Ji J. Zhang Y. Wu W. Liu Y. Lin L. Feng X. (2014). Regio- and Enantioselective Baeyer–Villiger Oxidation: Kinetic Resolution of Racemic 2-Substituted Cyclopentanones. *Org. Lett.* 16: 3938–3941.
- [Zoubir et al., 2017](#) – Zoubir M, Zeroual A, El Idrissi M, El Haib A, Moumou M, Hammal R, Mazoir N, Benharref A, El Hajbi A. (2017). Understanding the Chemoselectivity and Stereoselectivity in Michael Addition Reactions of β -Hydroxyparthenolides and Amines such as Pyrrolidine, Morpholine, Piperidine and 1-Methylpiperazine: a DFT Study, *Journal of Materials and Environmental Sciences.* 8: 990-996.